Master's Final Thesis

Master's Degree in Automatics and Robotics (MUAR)

High temperature proton exchange membrane fuel cells control for combined heat and power applications

July 2019

Author: Guillermo Lopez Diest

Directors: Ramon Costa Castelló

Escola Tècnica Superior
d'Enginyeria Industrial de Barcelona

Summary

Over the last few years, the research of new energy sources as a substitute for the current depletable ones has been increasing. One of these possible sources is hydrogen, one of the most common elements in the planet. By using what's called as a fuel cell, it can be used to efficiently generate clean electrical and thermal energy, as the only output is water.

This project has been developed in the framework of the DPI2015-69286-C3-2-R MICAPEM (Parameter estimation, diagnosis and control for the improvement of efficiency and durability of PEM fuel cells) project, which aims to create an architecture and control of a system that will be able to supply electrical and thermal power to a typically-sized house using a Proton Exchange Membrane Fuel Cell working at high-temperature (HT-PEMFC).

To do so, a Model Predictive Control (MPC) will be used, capable of controlling the amount of hydrogen being consumed based on the prediction of the house's electrical and thermal demand.

The numerical computation system Matlab will be used for the creation of the MPC and its Simulink tool, to model the PEMFC system. Then a series of simulations will be run, which will both test the controller in several scenarios as well as to understand its behaviour.

Contents

Chapter 1

Introduction

Nowadays, most of the energy consumed comes from petroleum, natural gas and carbon. However, concerns about the depletion of the fossil fuels, as well as contamination and climate change, have been increasing. This has resulted in the research of new clean energy sources that will be able to substitute them. This is of utmost importance in Spain, where the other current sources are either socially rejected, as its the case of nuclear plants, or, in the case of hydroelectric plants, are about to reach its limits.

Additionally, of all the types of energy consumed, the electrical and thermal ones are the most common ones. Therefore, part of the focus is placed in the search of new energy sources that will be able to produce both types while doing so both efficiently and in a clean way.

Fuel cells are one the best candidates to do so. These devices are electrochemical elements that use hydrogen as a fuel, generating electricity, heat and water, which can be cleanly outputted to the atmosphere. These can be used to only produce electrical energy, dumping the thermal into their surroundings, or in cogeneration, utilizing both electrical and thermal energy, arriving at 90% efficiency [1].

This master's thesis has been done as part of the MICAPEM project, that aims to create the first Spanish prototype microCHP-unit suitable for installation in the residential sector. To do so, a specific type of fuel cell was used, the High-Temperature Proton Exchange Membrane Fuel Cell (or HT-PEMFC).

1.1 Objectives

Being part of the MICAPEM project, the objective of this master's thesis is the design of a system capable of supplying both the electrical and thermal demand to a house utilizing the HT-PEMFC.

First of all, the mathematical model of the fuel cell will be created. Then, from such model, an analysis will have to be made to see what additional elements will be needed in order to ensure the correct supply of both demands.

Next, a controller will be used that will decide the amount of intensity the PEMFC will need to produce. Due to the periodicity of the demand as well as the desire to minimize the amount of hydrogen utilized, a Model Predictive Control will be implemented.

Lastly, the controller will be tested via simulation. It is important to remark that the objective isn't to design the system for a specific real house, but rather use the demand as a general one to test the different possible scenarios that the controller will have to face.

1.2 State of the Art

A fuel cell is an electrochemical device that transforms chemical energy into electrical and thermal one. They are based in a reaction where a fuel, which tends to be hydrogen, reacts with an oxidant generating energy. The oxidants, such as oxygen, can be taken directly from the atmosphere, removing the need to store them, and needing only to worry about the hydrogen.

The principle on which fuel cells are based was discovered in 1839 by William Grove but the development of thermal machines shadowed the progress of fuel cells. However, over the last decades, concerns about the depletion of the natural resources along side the desire to reduce contamination and climate change have increased. This has resulted in more research done of fuel cells, due to their zero emission generation during the electrolysis, as its product is water, which can be outputted directly to the atmosphere.

Fuel cells currently have a series of advantages over other current energy sources [2]. As it was just mentioned, they have very little emission of polluting particles. Additionally, they have a high efficiency, reaching up to 85% in cogeneration, produce much less noise, and at the same time are scalable, as they be stacked on one another, and require low maintenance.

However, the current drawbacks outweight the advantages fuel cells provides. First of all, the initial cost needed to implement a functioning system is very high, which is one of the main variables costumers take into account. Also, hydrogen storage is a very important problem [3, 4]. Currently, the implemented storages tend to be inefficient and slow when required to get hydrogen in and out of the container. Additionally, they tend to be voluptuous, heavy, costly and not very durable.

All this disadvantages highly increment the cost of the utilization of hydrogen. However, when compared to fossil fuels, the main disadvantage it faces nowadays is the lack of proper standards during its production and storing, as well as the lack of infrastructure surrounding this technology, which limits the amount of reach it was in the society.

Nowadays, research is focused on the reduction of the cost in both the storage and hydrogen production, as these are the two more costly steps, as well the improvement of the efficiency of fuel cells.

While hydrogen is one of the most common elements, it is never in an isolate state, having to be produced via a chemical reaction [5, 6, 7]. Depending on its source, the use of hydrogen can be qualified as either renewable or non-renewable energy.

Figure 1.1 shows the different processes that result in this element, being biomass, electrolysis

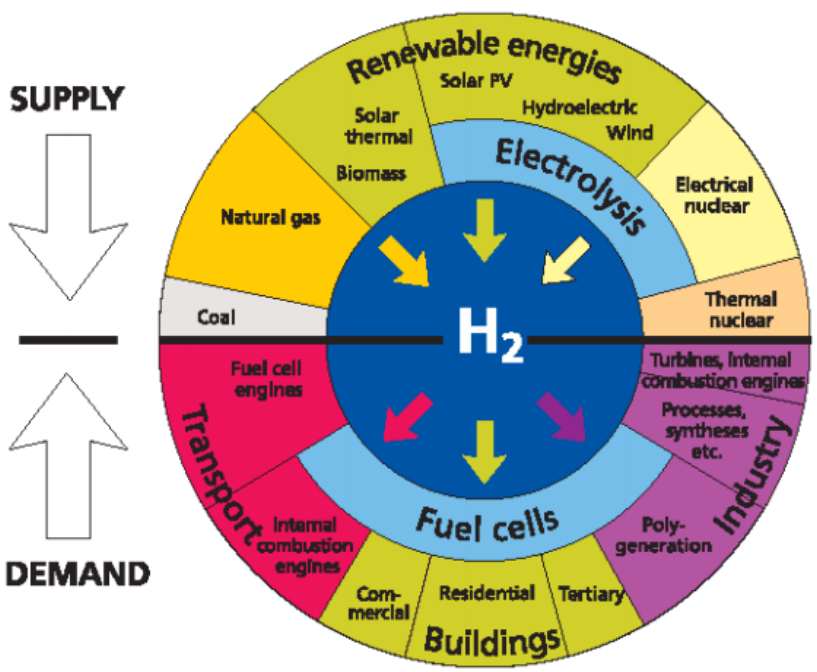

Figure 1.1: Hydrogen production and applications diagram. [6]

and hydrocarbon reforming the most important ones. First of all, the fermentation of biomass [8], which is a renewable source of hydrogen. The sources of biomass are very diverse, being the waste and residues created in forestry, agriculture, industry and cities. When heated, this products decompose into hydrogen, carbon monoxide, methane and other product such as oils or tar:

$$Biomass + heat \rightarrow H_2 + CO + CH_4 + others.$$

Then, what's called as hydrocarbon reforming can also be used, the reaction of a hydrocarbon with high-temperature steam to produce hydrogen and carbon monoxide. This CO can again be reacted with more steam to produce hydrogen and carbon dioxide. Molecules that are based on the addition of oxygen to the hydrocarbons will directly produce carbon dioxide and hydrogen:

$$CH_4(g) + 2H_2O(g) \rightarrow CO(g) + 3H_2(g) + H_2O(g) \rightarrow CO_2(g) + 4H_2(g)$$
$$CH_3OH(g) + H_2O(g) \rightarrow CO_2(g) + 3H_2(g).$$

Lastly, electrolysis can be used, which is based in the use of an electrical current to split the water molecules into hydrogen and oxygen:

$$2H_2O(l) \rightarrow 2H_2(g) + O_2(g).$$

Chapter 2

Proton Exchange Membrane Fuel cells

In order to be able to supply the necessary demand to the house, several different elements will have to be used. The main one is going to be the Proton Exchange Membrane Fuel Cell (PEMFC), used to produce the necessary energy consumed by the electrical and thermal demand. It is therefore important to understand in detail what is its behaviour.

2.1 General Concepts

A fuel cell is an electrochemical element capable of generating electrical and thermal energy from the chemical energy produced by an specific chemical reaction. One can be seen in figure 2.1.

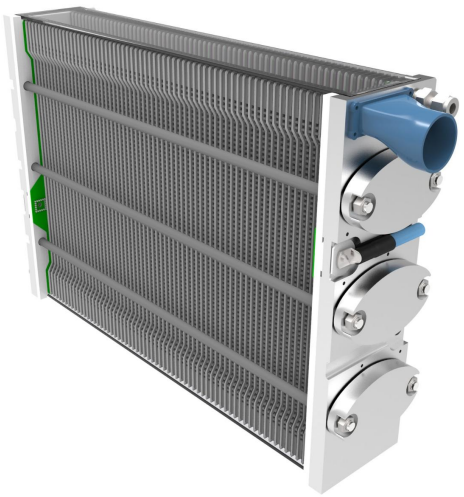

Figure 2.1: Fuel cell stack [9]

There are currently several types of fuel cells [10], depending on the chemical fuel used in order to generate the electrical energy. Nowadays, the most common ones are the Alkaline Fuel Cells (AFC), Proton Exchange Membrane Fuel Cell (PEMFC), Direct Methanol Fuel Cell (DMFC) and the Phosporic Acid Fuel Cell (PAFC).

When comparing several types of fuel cells, one of the common products the chemical reactions produce is water. Despite existing several classification methods, this fact is used to differentiate between two different types of fuel cells, high and low temperature ones. When talking about high temperature, it is normally referred to as fuel cell working above the boiling temperature of the water, being the product of the chemical reaction steam, instead of liquid water. While the chemical behaviour is the same in both cases, this difference drastically changes the physical components of such cells, which have to be adapted to the extraction of either liquid water or steam.

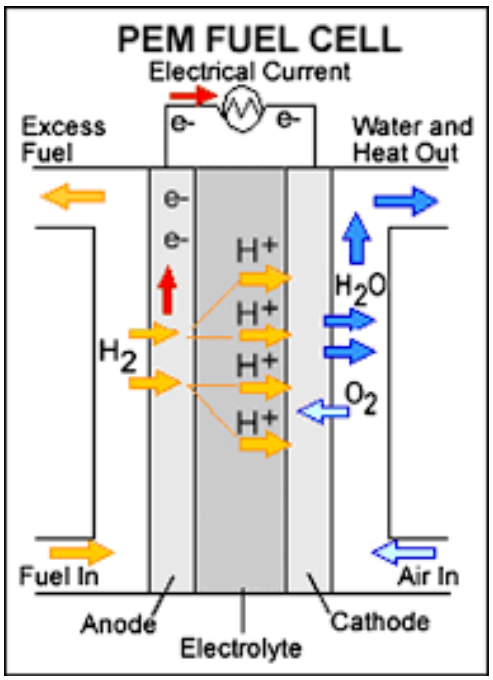

Figure 2.2: Diagram of the gas flows in a PEMFC [11].

Figure 2.2 shows an schema of the different flow of elements in a PEMFC. For this type of cell, the fuel used is hydrogen, which enters the cell via a conduct in the anode side, seen in the left side of the figure. When the hydrogen comes in contact with the electrode, it dissociates itself into protons and electrons. As hydrogen gas is composed of biatomical molecules, 2 protons and 2 electrons will be generated per molecule. The electrodes tend to be covered by platinum, that acts as a catalyst.

In order to ensure the maximum usage of hydrogen, two operating modes are used. First of all, the Dead-End Anode mode closes the outflow of hydrogen, opening it only to ensure the renovation of the hydrogen, which purges some particles of water and nitrogen present in the anode as well as a small amount of hydrogen left. The second one, called feedback mode, recirculates the hydrogen that hasn't reacted back into the anode.

On the other side of the system, oxygen comes through the cathode's side, and in conjunction

with the dissociated hydrogen atoms, reacts generating water. This reaction is exothermic, releasing energy when it occurs.

$$H_2(g) \rightarrow 2H^+ + 2e^-$$
$$\frac{1}{2}O_2(g) + 2H^+ + 2e^- \rightarrow H_2O(g)$$

$$H_2 + \frac{1}{2}O_2 \rightarrow H_2O \tag{2.1}$$

To transform this chemical energy into electrical one, a specific type of membrane is placed between the anode and the cathode, that only allows the flow of protons, giving the name to the fuel cell. Therefore, the electrons have to take the longer path, travelling through the electric cable between the anode and the cathode, producing the electrical energy sought for.

2.2 Model of a PEMFC

2.2.1 Chemical voltage

The first step in order to calculate the amount of energy produced by the fuel cell is to know how much energy does the reaction produce. In chemistry, this is called as the enthalpy of reaction and is calculated from the enthalpy of formation of the reactants and products present in the reaction. For standard condition, 1 atm and 298K, these are already tabled.

By definition, in standard conditions, the enthalpy of formation of elements is 0 KJ/Kmol, which include O_2 and H_2. As for steam (as it is a high temperature fuel cell), it has a value of -241,820 KJ/Kmol. The negative value represents that the reaction is exothermic, or in other words, that liberates energy when it occurs. Therefore:

$$\Delta H = \Delta f H_{H_2O} - \frac{1}{2}\Delta f H_{O_2} - \Delta f H_{H_2} = -241,820\frac{KJ}{KmolH_2O}.$$

Note the one-half multiplying the oxygen's enthalpy. This is due to the stoichiometry of the reaction, as only half mol reacts, seen in (2.1). From this enthalpy, the chemical voltage can be calculated, which will give the maximum theoretical voltage the fuel cell can provide:

$$\Delta H = -V_q nF,$$

being V_q, the chemical voltage, n the number of electrons in the hydrogen molecule, which is two, and $F = 96485Q/mol$, the Faraday constant. Here, the stoichiometry is also important, as the enthalpy of the reaction is expressed in KJ per mol of water. This has to be changed to mols of hydrogen, seen in the second term of (2.2). With this in mind, the chemical voltage is:

$$V_q = \frac{-\Delta H}{nF} = \frac{241,820 \frac{KJ}{KmolH_2O}}{296.485 \frac{Q}{KmolH_2}} \frac{KmolH_2O}{KmolH_2} = 1.253V \tag{2.2}$$

As this voltage is in general not enough to supply power to possible applications, two or more fuel cells are stacked with one another, which results in a final voltage proportional to the amount of cells used.

However, this was just an example of the chemical voltage calculus as two important simplifications have been made, which directly affect its value.

Gibbs free energy

According to Josiah Willard Gibbs' free energy equation, not all of the chemical energy produced in the reaction is extractable, as some is lost to the universe, increasing its entropy. As a result, not all the enthalpy will be used, having to substitute the enthalpy in (2.2) by (2.3), which will lower the chemical voltage produced.

$$\Delta G = \Delta H - T\Delta S, \tag{2.3}$$

with T the temperature of the fuel cell and ΔS the entropy.

Nerst equation

Lastly, all the previous calculus have been done supposing standard conditions (1 atmosphere, 298 K), but this isn't going to be the case inside the fuel cell. To calculate more accurate value of the Gibbs energy, a small readjustment has to be made:

$$\Delta G = \Delta G^0 - \frac{RT}{nF} ln(Q),$$

with T the temperature of the fuel cell. $R = 8.3144 J/molK$, and $F = 96485 Q/mol$ are the gas and Faraday constants respectively. Q is the reaction coefficient of 2.1, which is defined as the multiplication of the product's coefficients divided by the reactant ones. As all the components are gaseous, this coefficients can be changed to the partial pressures:

$$Q = \frac{P_{H_2O}}{P_{H_2} P_{O_2}^{0.5}}.$$

The oxygen will be taken directly from the atmosphere, so it will have a partial pressure of 0.21 atm, and the produced water will be at 1 atm, as it is expelled into it.

As a reference, at a temperature of 150ºC, and taking into account both the Gibbs free energy as well as the Nerst equation, this will result in a chemical voltage of 1.15 V.

2.2.2 Polarization curve

While the theoretical voltage gives an approximation of the electrical voltage that the fuel cell will produce, not all of the chemical energy will be converted into electrical one, as there are bound to be energy losses inside the fuel cell that will reduce its efficiency. In general, all these losses are computed experimentally, but from a theoretical point of view, they can be differentiated in three types, the activation losses, the diffusion (or concentration) ones and the ohmic [12, 13].

Activation losses

The first type of losses are the activation ones, which are caused due to the need of a difference in voltage at anode and cathode for the reactions to occur.

From the two reactions, the voltage needed to start the oxidation of the hydrogen is usually ignored as it in negligible when compared with the oxygen's reduction. These losses are important at low intensities, but due to its logarithmic nature, they can be supposed constant for higher values:

$$V_{act} = \frac{RT}{\alpha nF} ln(\frac{i}{i_0}), \tag{2.4}$$

where α is the transfer coefficient, i the fuel cell's current density and i_0, the exchange one.

Ohmic losses

The next important losses are the ohmic ones, given by the resistance of the different elements of the system to the flow of electrons. Of all the elements, the two most important ones are the membrane and the electrodes:

$$V_{Ohmic} = I(R_m + R_c), \tag{2.5}$$

with R_m the membrane resistance and R_c the electrode's one.

Diffusion losses

Lastly, when the intensity that flows through the fuel cell is high enough, the rate at which the hydrogen molecules react is so fast that the inflow of fuel isn't capable of keeping up, as its dynamics are much slower, resulting in a gradient of concentration that creates a drop in voltage. This is specially important in points of the cell where the hydrogen takes longer to reach and are the most important losses at high current density:

$$V_{conc} = -\frac{RT}{nF} ln(1 - \frac{i}{i_l}), \tag{2.6}$$

with i_l the limit current density that results in a null net voltage.

Mathematically, the electrical voltage that the fuel cell will produce, can be calculated as:

$$V_{fc} = E_{th} - V_{act} - V_{ohmic} - V_{conc}, \tag{2.7}$$

where, ,V_{fc} is the fuel cell's voltage and E_{th}, the chemical voltage produced by the hydrogen reaction taking into account both the Gibbs free energy and the Nerst equation.

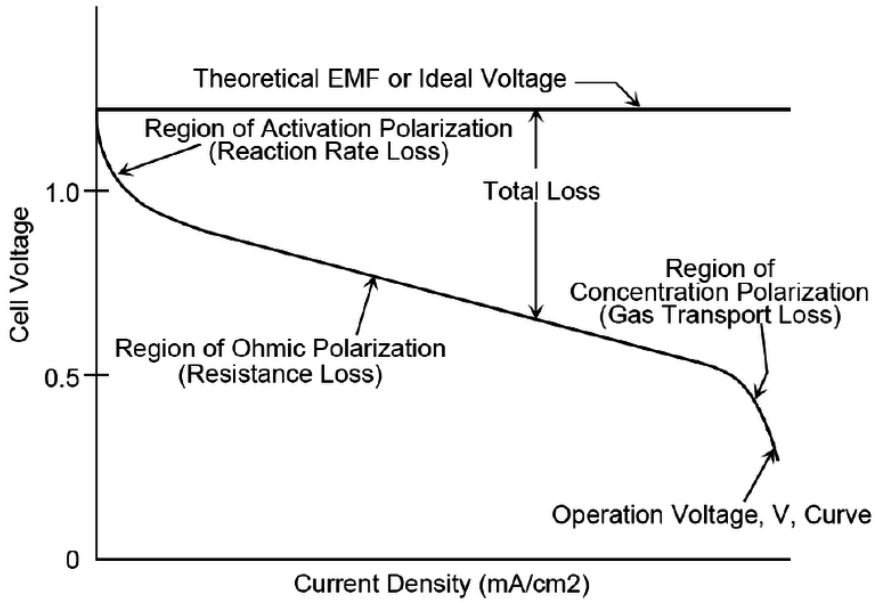

Figure 2.3: Polarization curve of a PEMFC with the different regions [14].

As all the theoretical formulas are expressed as a function of the current that flows through the fuel cell, a graph can be made, that shows the relation between the intensity, or current density, in the horizontal axis and the voltage of the cell, in the vertical one. This is what's called as a polarization curve and figure 2.3 is an example of one.

Three clear regions can be seen from the graph. While the three theoretical losses create a voltage drop, depending on the amount of current density, one of them will dictate the behaviour of the fuel cell at an specific zone. As it was previously stated, the activation losses are the most important ones at low currents and the concentration ones, at high intensity. Due to the logarithmic nature of the two, at medium density current values, they can both be considered constant, and the change of the electrical voltage is caused by to the ohmic ones.

2.2.3 Effect of the temperature

It is also important to note that the losses inside the system are dependent on the temperature. As it rises, the activation voltage decreases, as well as increasing the conductivity of the membrane and electrodes, reducing the overall losses and increasing the electrical voltage outputted by the fuel cell. Figure 2.4 shows an example of the changes in the curve for different temperatures.

As a result, in order to achieve a better fitted model, the resulting outputted voltage can be multiplied by a factor close to 1. However, this isn't normally used, as controlling the temperature requires a lot of fine tuning in elements such as the refrigerating system, while vastly increasing the control difficulty. Additionally this is only useful when trying to maximize the efficiency working in co-generation, but results only in a slight improvement in performance. For most of the cases, the fuel cell is kept stable at a certain temperature and as the electrical voltage tends to be calculated experimentally, the temperature factor isn't needed.

Figure 2.4 shows the effect of the temperature in the polarization curve, having a higher electrical voltage the higher the fuel cell's temperature.

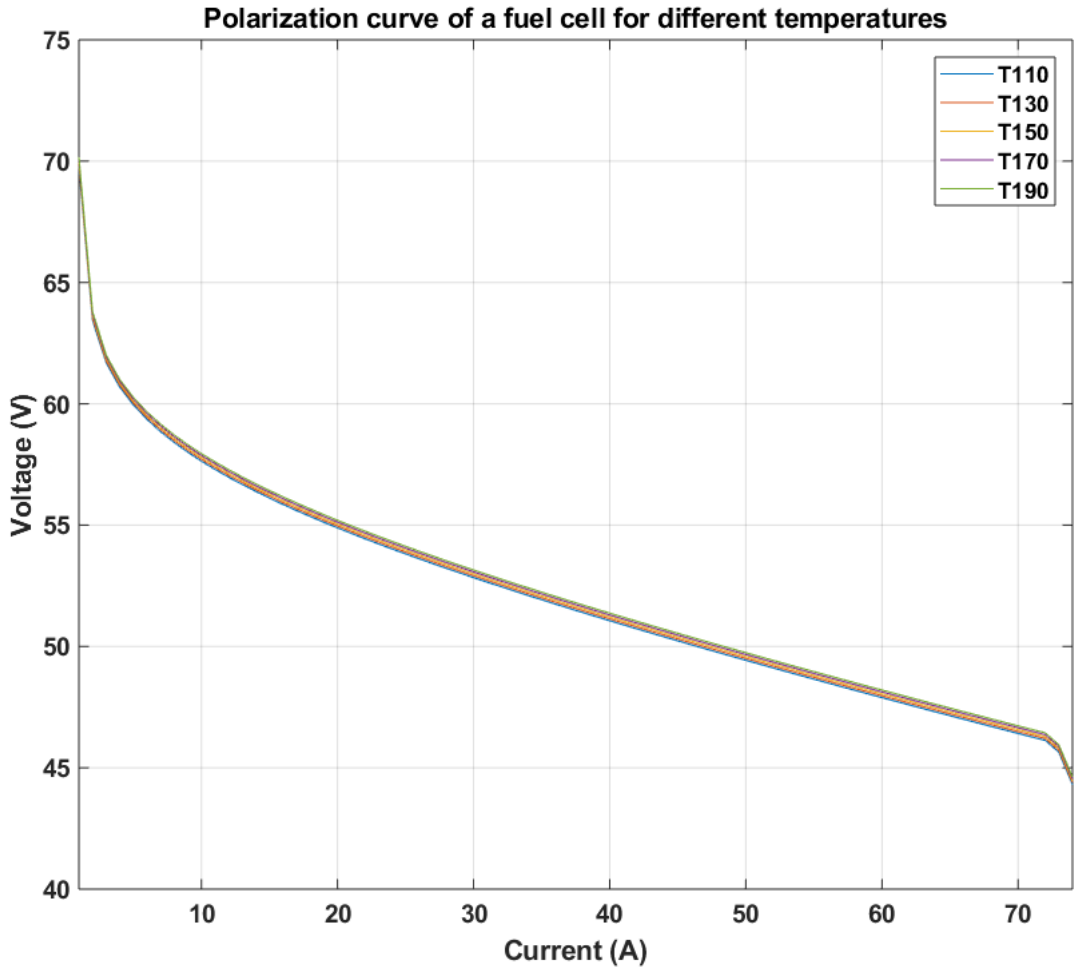

Figure 2.4: Effect of the temperature in the polarization curve.

To create the different curves, the model seen in figure 2.5 was used. On the left, the model of the fuel cell is seen, and on top of it, a block that calculates the needed hydrogen flow to produce the desired intensity. These blocks will be explained in detail in section 3.2.1. In the middle, a current source forces the current of the fuel cell to a certain value and it goes from zero to the maximum intensity value of the fuel cell, the maximum value of the fuel cell's intensity. Lastly, on the right, the voltage, current and chemical voltage of the cell are stored, to later on plot them. This schema has also been used to calculate the electrical and thermal power curves,

seen in section 2.4.

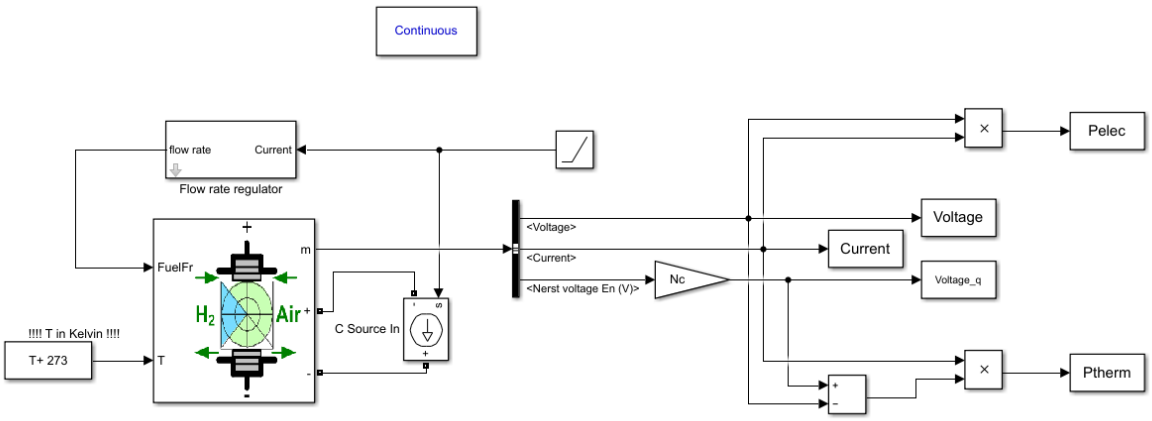

Figure 2.5: System used to create the different PEMFC curves.

2.3 Hydrogen flow to intensity

Due to the chemical nature of the system, the relationship between the amount of hydrogen inflow is directly connected with the current produced. As each molecule of hydrogen dissociates in 2 electrons, the amount of current density is:

$$i = nFq_{H_2}, \tag{2.8}$$

where q_{H_2} is the flow of hydrogen, in mol/cm^2s. Multiplying by the area of the hydrogen flow, the Intensity will instead be calculated.

As it will be explained later on, the hydrogen won't be the variable controlled, but rather the current that flows through the cell. Therefore, the expression searched for isn't the intensity as a function of the hydrogen but hydrogen as a function of the current:

$$q_{H_2} = \frac{i}{n_e F}. \tag{2.9}$$

2.4 Electrical and thermal power

As the polarization curve relates the voltage of the cell with the intensity, the electrical power generated can be rapidly calculated, as it is the product of the voltage by the current. Additionally, as all the chemical power that hasn't transformed to electrical will have heated the system, the thermal power can also be calculated:

$$P_{elec} = V_{fc} I_{fc}$$
$$P_{ther} = (V_q - V_{fc}) I_{fc},$$

with V_{fc} and I_{fc} the voltage and current of the fuel cell respectively, and V_q the chemical voltage of the cell.

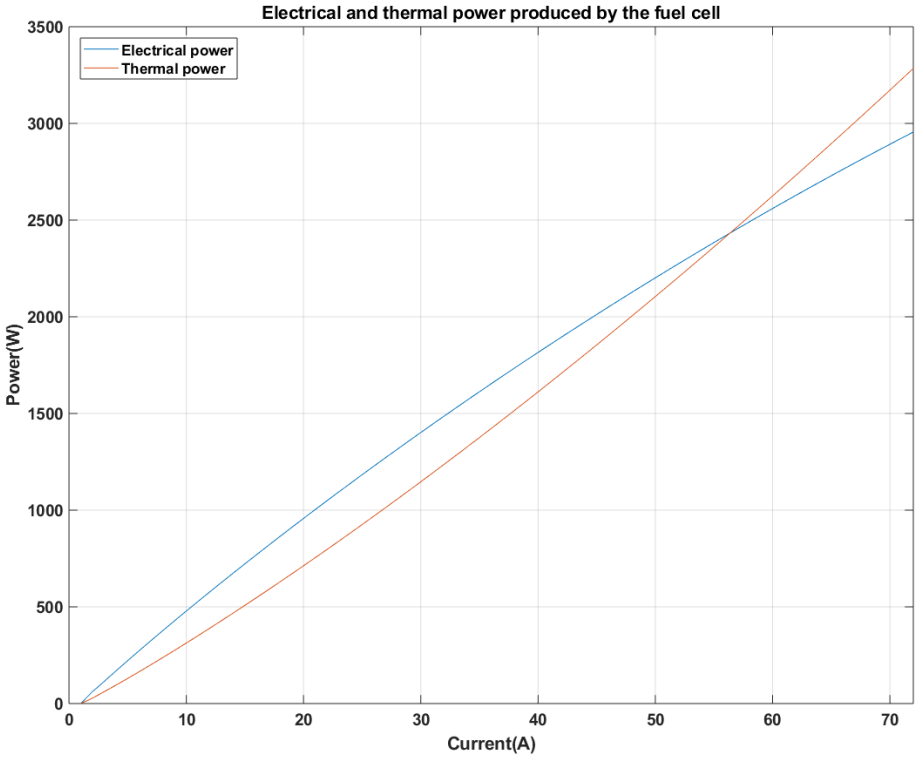

Figure 2.6: Electrical and thermal power generated by a fuel cell dependent on the intensity

Figure 2.6 shows both the electrical and thermal power generated by the fuel cell. For low currents, the electrical power generated is larger than the thermal one. This remains true up to a point, where the thermal power surpassed the electrical one.

2.5 Failure points and maintenance of PEMFCs

The last point needed to take into account are the possible failure point as well as the correct maintenance of PEMFCs [15], to ensure the maximum efficiency of the cell.

Regarding the failure points, they tend to be classified into 5 different possible ones. Focusing on the physical components of the cell, two defects are membrane related. The first one is the dehydration of the membrane, which can cause the incorrect functioning of the membrane, as the capacity of conducting protons is highly related to the amount of water. To avoid this problem, the fuel should be humidified.

Moreover, physical defects in the membrane may cause the mixing of hydrogen and oxygen in the cell, which might chemically combust, increasing the leak size. One of the key factors in PEMFC research is the creation of better membrane that minimize this effect.

Also, the electrodes can also be poisoned by carbon monoxide. This is specially important at lower temperatures and over time, it will cause the degradation of the catalyst and with it, the loss of efficiency. By periodically using high pulses of current, this is hugely reduced.

Lastly, the two final possible failure points are hydrogen related. Due to its nature, the fuel cell is bound to have some hydrogen leaks into its surroundings, which are normally accepted as losses. A huge amount of losses however, can dangerously increase its concentration, which can cause its combustion. Additionally, as the electric dynamic are much faster than the hydrogen flow ones, rapid increases in intensity can result in some areas having no hydrogen left, causing the cells degradation. This is specially important at places where the hydrogen flow takes longer to reach such as tight corners.

While some of these failures have a possible solution, fuel cells in general don't have an established maintenance protocol that will ensure its durability.

Chapter 3

System

In this chapter, the system used will be analyzed, starting with its architecture along with the reasoning behind its choosing. Then, the models of the different elements of the system will be explained in-depth. Finally, the mathematical model of all the system will be calculated.

3.1 Architecture of the system

When trying to supply both electrical and thermal demands, it can be clearly seen that the fuel cell alone isn't capable of doing so, as both types of power are dependent of each other, while the demands aren't. This requires the use of storing elements between the loads and the cell. Figure 3.1 shows the system's architecture, which will be now explained.

For the electrical part, a battery will be the element used. The fuel cell, battery and electrical load have been connected to the same grid, and a PI controller will ensure that its voltage remains at a constant value. As a security measure, a connection is available between the system's grid and an external one, in case the battery needs an emergency recharge or discharge.

In the thermal part, a water tank will be used as the heat accumulator, storing the thermal energy produced. Additionally, an exchanger will have to be used to extract the thermal energy produced by the cell. This exchanger will be a tank of oil where the cell will be submerged in, and with the recirculation of this oil, the thermal power will be transferred to the heat accumulator. This oil tank can be seen in figure 3.2.

Same as with the battery, a security element has been placed, to avoid the water in the tank from boiling. This can be done by replacing a part of the hot water with colder one via a series of valves, effectively resulting in the loss of this hot water's thermal energy.

Lastly, a resistance has been placed in the water tank, and utilizing the Joule effect, it functions as an easy way to transform some of the electrical energy into thermal one.

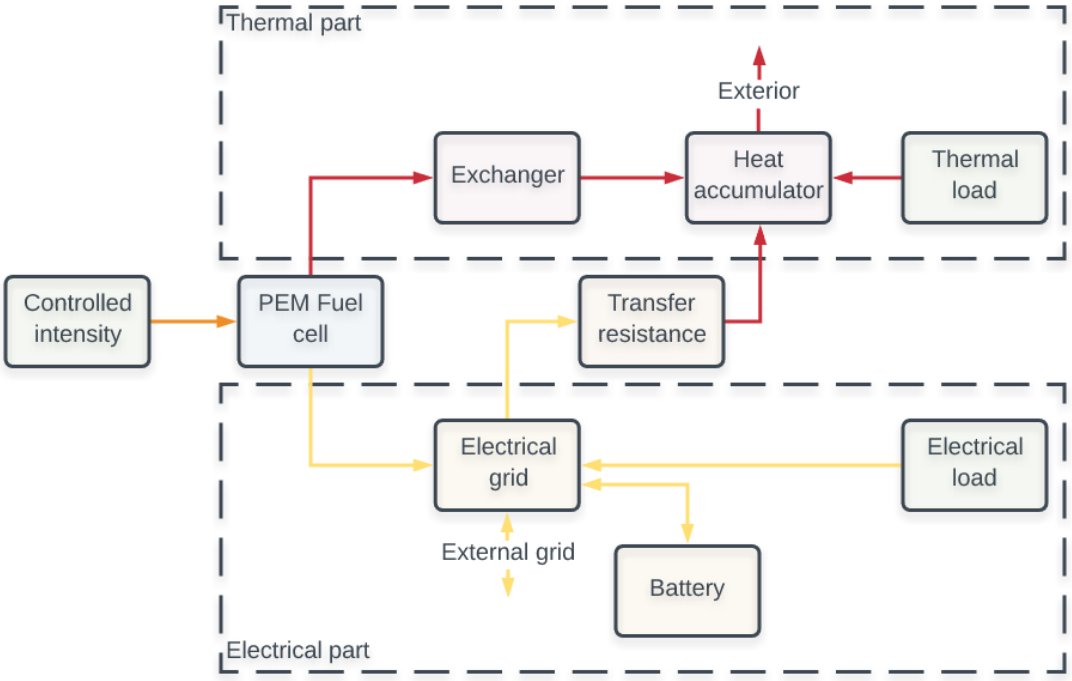

Figure 3.1: Architecture of the system.

Figure 3.2: PEMFC's Oil tank.

3.2 Modelling of the elements of the system

Following the ideas behind the architecture explained in the previous section, a model of the system was created, which can be seen in figure 3.3. This modelling was done using Matlab's Simulink tool.

The lower part of the system represents the electrical part. Starting from the left, the fuel cell's block can be seen, which is connected to the electrical grid. Two additional elements are also connected to this grid, the battery, in the middle and the electrical load, on the right. A capacitor is set in the grid to keep it at a constant value.

On the other hand, the upper part corresponds to the thermal part, being both the exchanger and heat accumulator grouped in the purple block in the middle.

The green boxes represent all the different inputs of the system and the red ones, the output. A breakdown of the element blocks will be done in the next sections.

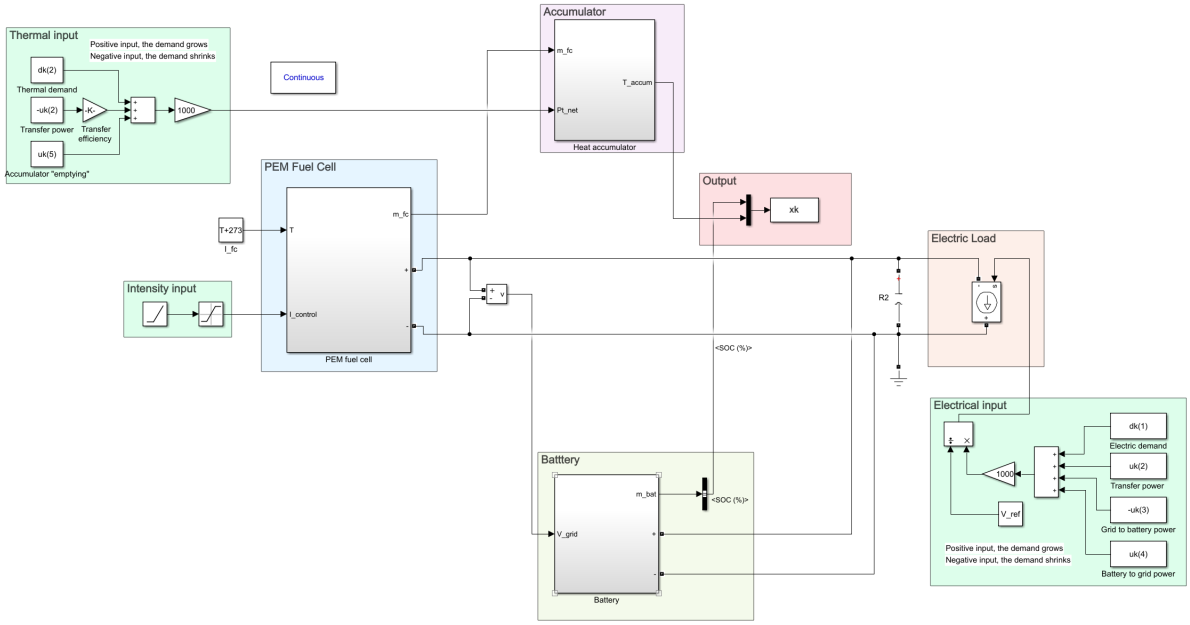

Figure 3.3: Simulink model of the system.

3.2.1 Proton Exchange Membrane Fuel cell

Starting with the energy generator, the fuel cell, figure 3.4 shows the configuration of the PEMFC. It is important to note that the input to the fuel cell will be the intensity, decided via the controller. In figure 3.3 the intensity is modelled as a ramp. As it was explained in section 2.5, this is due to the fact that big changes in intensity highly increasing the deterioration of the cell. Therefore, the input intensity change is set to a fixed value of 1 A/s, going from the previous control value to the new one calculated by the controller.

From the figure, three elements can be distinguished. On the left, the model of the fuel cell.

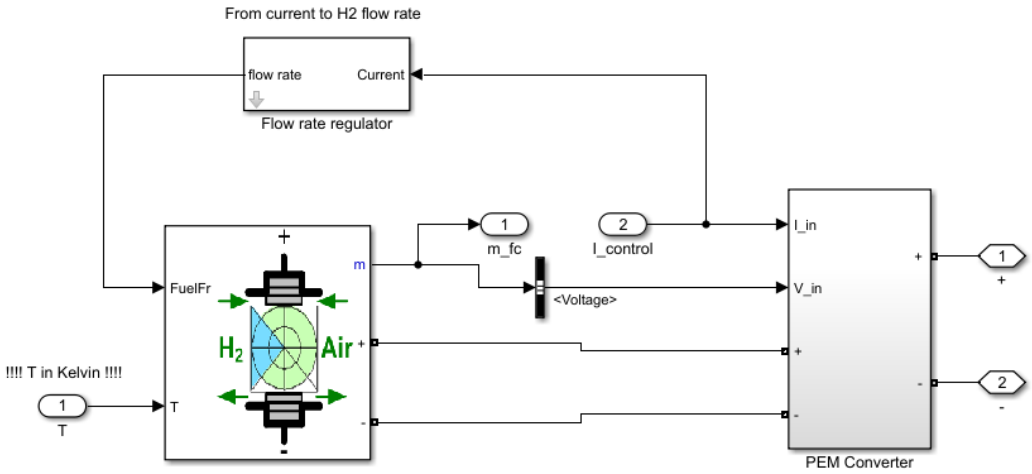

Figure 3.4: Fuel cell Simulink model block.

Then, on the right, a converter has been placed, that connects the cell with the external grid. Lastly, a block has been created, designed to input the amount of hydrogen needed, dependent on the desired intensity.

The model of the fuel cell has been done using the *Fuel cell* model of the *Simscape toolbox*. By clicking on the model, all the information is displayed (see figure 3.5). There, the parameters of the fuel cell can be set, having a total of 6 predefined fuel cells available. If the *Model detail Level* is set to *Simplified*, only the first 3 will be displayed, which correspond to the creation of the polarization curve of the fuel cell. If, on the other hand, it is set to *Detailed*, the rest of the options will appear, as well as the *Signal variation* window, which allows the change of the parameters of the fuel cell over time via inputs to the model.

Then, on the right side, the model of a converter has been created. Due to the fuel cell's voltage being a function of the intensity, a converter is needed before outputting the produced energy into the grid. As the voltage of the fuel cell is lower than the grid, the converter used will have to be a boost type.

Physically, a converter is able to output a constant voltage due to a fast-switching. While modelling this behaviour isn't very complicated [16, 17], the simulations tend to take much longer due to such nature. In the end, a converter can be simplified to an energy balance equation, such that the power inputted is the same as the outputted, except a small fraction, due to internal losses:

$$V_{out} I_{out} = \mu_{conv} V_{in} I_{in}.$$

For this master's thesis, the output voltage is the grid's one, which is a constant value. Additionally, the input variables are known, as the intensity will be given by the controller and the voltage, fixed by the intensity. This allows the calculus of the output intensity of the converter. The created converter model can be seen in figure 3.6.

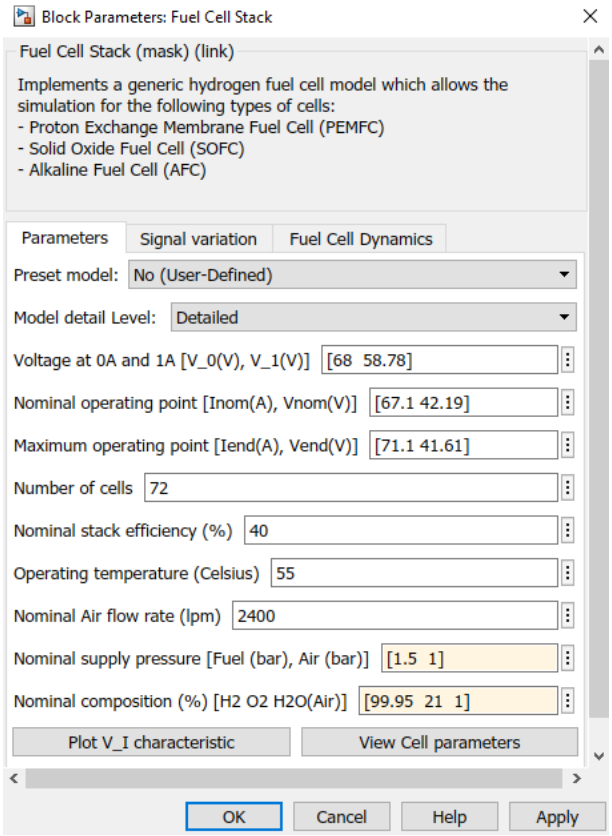

Figure 3.5: Details of the PEMFC's model.

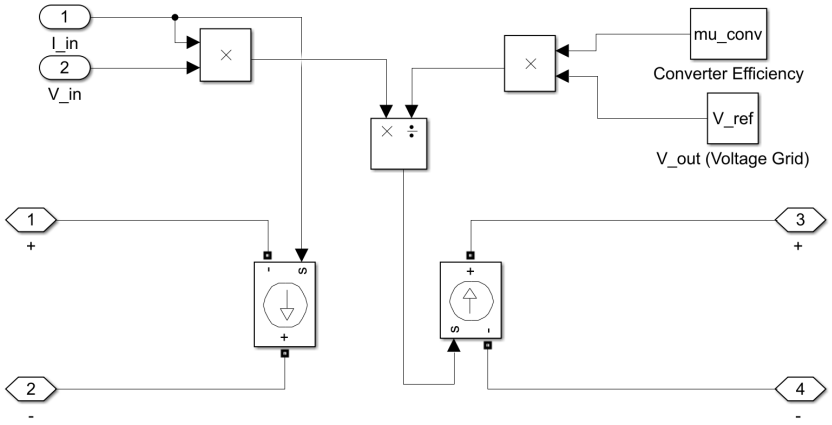

Figure 3.6: Simulink converter model

Lastly, the controller will set the cell's intensity to a given value, but this has to be converted to hydrogen flow. Internally, the Simulink block in figure 3.4 is just a function, which can be seen in (3.1).

This equation is based in (2.9), being the second term of (3.1). These calculates the hydrogen needed in mol/s, but the Simulink model's input is the amount of fuel in l/min. To pass from hydrogen to fuel, the hydrogen utilization and composition, $H_{2_{comp}}$ and $H_{2_{util}}$ respectively, are used, seen in the first term. With the third term, the mol/s are changed to m^3/s and thanks to

the 60000, to l/min. The number of cells, N_c are also taken to account.

$$q_{H_2} = \frac{60000 N_c}{H_{2_{comp}} H_{n_{util}}} \frac{I}{2F} \frac{RT}{P_{fuel}}, \tag{3.1}$$

where T is the fuel cell's temperature in Kelvins, P_{fuel} the pressure of the hydrogen and R, the gas constant, of $8.314 J/molK$,

3.2.2 Battery

The second element that has been modelled is the battery. From figure 3.7, the battery model can be seen, on the left, which is again available at the *Simscape toolbox*. The block has 4 parameters: nominal voltage, rated capacity, initial state of charge and response time. Additionally, the battery discharge, temperature and aging effects can also be modelled.

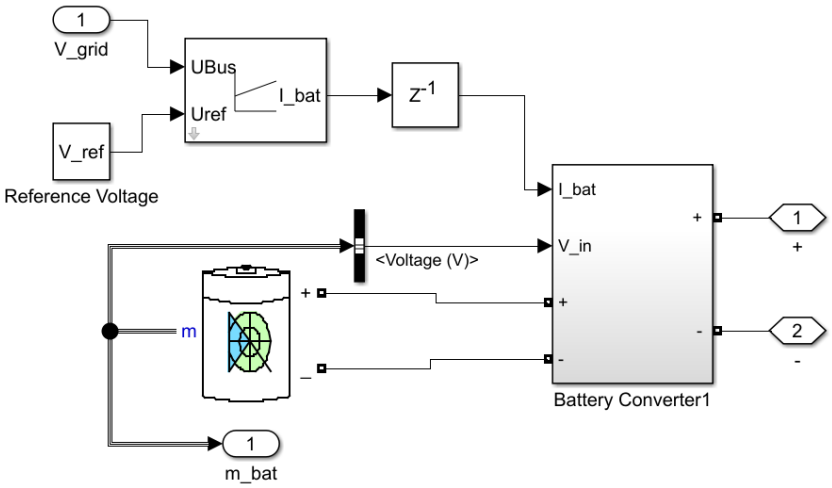

Figure 3.7: Simulink's battery model, converter and PI control.

Another converter has been created between the battery and the electrical load's grid, to boost the voltage to the reference one. In contrast with the cell's one, in this case the battery can be both charged and discharged, therefore the converter has to be bidirectional. This is modelled as a change in the efficiency of the converter, that will depend on the sign of the battery's intensity. Therefore, it was set to lower than one for positive battery currents and for the opposite case, the inverse of the efficiency was used, as the input intensity will now be the grid's one.

Additionally, to control the grid's voltage, a PI control has been set, which compares such voltage to the reference one and acts on the battery's intensity in order to maintain it at such value. It can be seen in the upper left corner of figure 3.7 and in detail in figure 3.9. A saturation has been placed in the output to avoid large intensities flowing through the battery. The calculus of the different parameters of the PI control will be explained in section 7.3.1. Lastly, as a quick note, a delay was added to the PI control as without it, Simulink detected a loop, not starting the simulation.

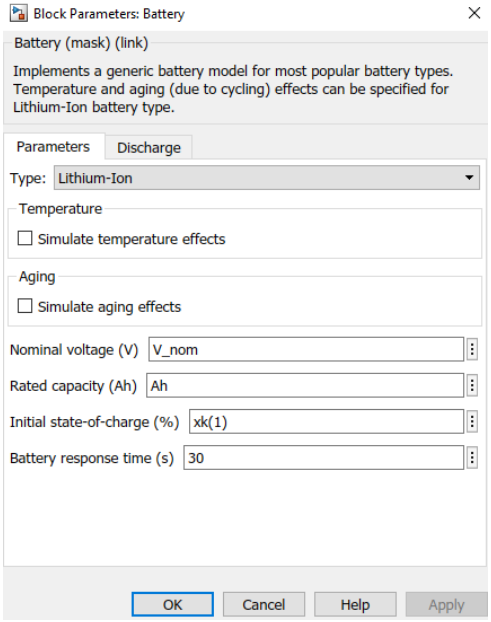

Figure 3.8: Details of the battery model.

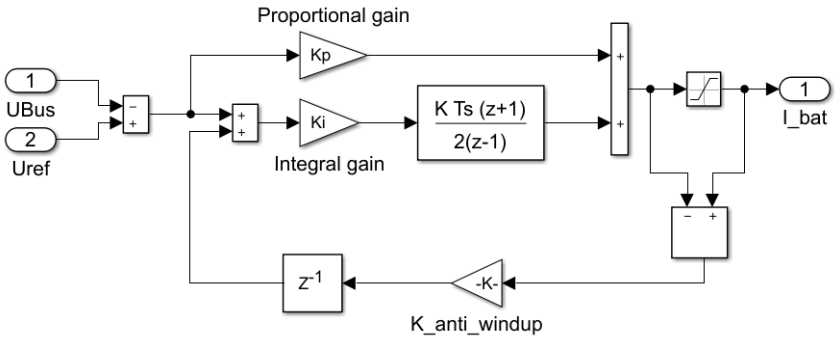

Figure 3.9: PI control model

3.2.3 Electrical load, inputs and security elements

To model the electrical load that the fuel cell will be subject to, a current source has been placed in the electrical grid. To calculate the intensity needed, the voltage of the grid should be used, dividing it by the demand, in Watts. However, to do so created a loop in the system, as the voltage grid determines the load's current which at the same time defines the voltage grid. This can be avoided by taking into account the grid's voltage as the reference one, and with a good PI control, this should always be true.

Additionally, three other inputs are modelled in the system, one being the electrical to thermal conversion and the other two, the security systems of the battery.

The amount of electrical power consumed by the resistance can be controlled by putting it in parallel to the electrical grid and varying the intensity that runs through it. As for the security elements, these exchanges depend on converters placed between the two grids and can also be easily controlled to produce the amount of desired power. Therefore, these three additional

inputs have been modelled as increases or decreases in the electrical demand of the system.

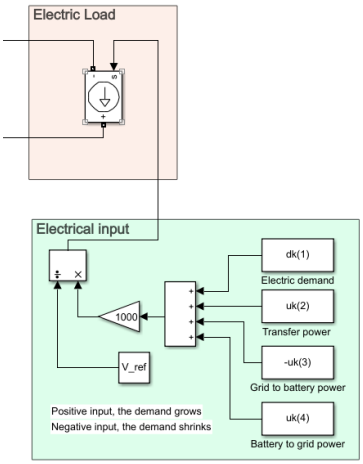

Figure 3.10: Electrical load, in red, and electrical inputs, in green.

3.2.4 Heat exchanger and accumulator

Starting with the thermal part of the system, a water tank is used as a simple way to store the thermal energy produced by the fuel cell. As the exchanger will be the oil tank surrounding the cell, it can be modelled just as a thermal power loss before arriving to the accumulator.

Figure 3.11 shows the calculus of the thermal energy produced by the fuel cell and the accumulator block model [18], seeing in figure 3.12.

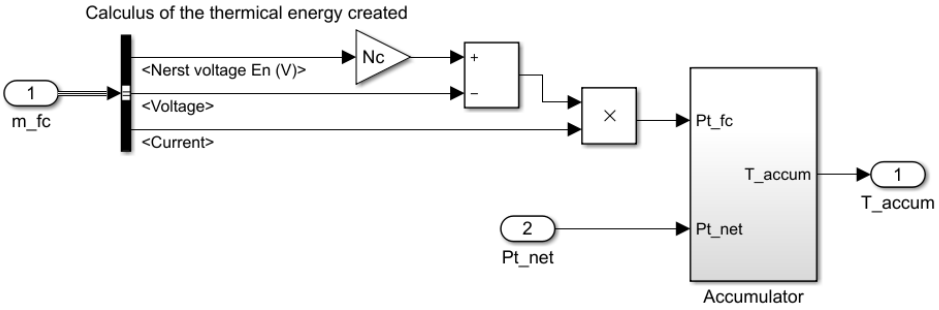

Figure 3.11: Thermal energy calculus on the left, and the accumulator block, on the right.

3.2.5 Thermal inputs and security elements

Lastly, the thermal inputs have been modelled. In this case, the model consists of a constant block with the demand value, that will be later subtracted to the thermal power produced by the fuel cell, seen in 3.11 as the Pt_net input.

Similar to the electrical case, the electrical to thermal transfer resistance has been modelled as an increase in the produced thermal power, being equal to the electrical power consumed, minus

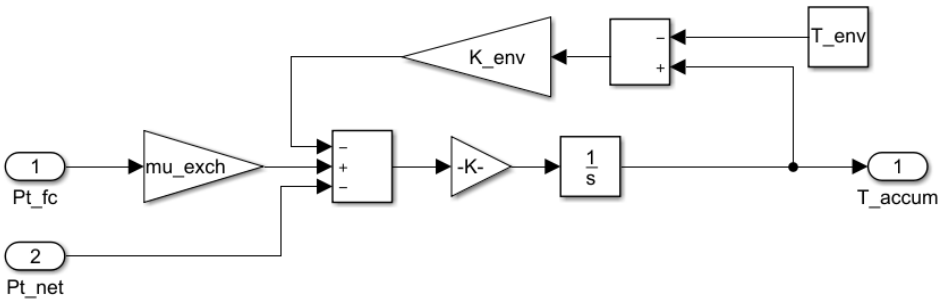

Figure 3.12: Model of the accumulator.

some losses. As the amount of hot water extracted from the tank can be easily controlled by a valve, this security element has also been modelled as a net power input, seen in figure 3.13.

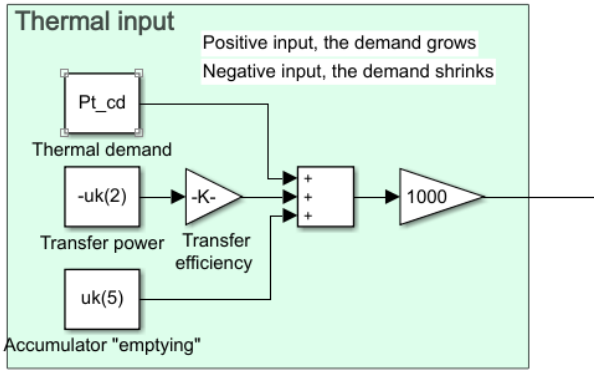

Figure 3.13: Thermal inputs of the system

3.3 Model

From the system, there is a clear differentiation of two parts, the electrical and the thermal one. Therefore, when modelling the system, at least two states will be needed, one to represent the electric part and another one for the thermal one.

In both cases, the stored energy in the battery and heat accumulator make perfect candidates as the state space variables of the system. This will be later seen that it causes numerical problem with the optimization problem, as the magnitudes of the different parameters are too different. To solve this, the state space variables have been changed to the State of Charge (SoC, in %) of the battery and the temperature (T, in Celsius) of the heat accumulator, which are proportional to their respective stored energies.

As initially, the energy stored were used as state space variable, two energy balances were calculated to model each part. The general expression of an energy balance is:

$$\frac{dE}{dt} = P_{in}(k) - P_{out}(k),$$

but as the system will be controlled with a Model Predictive Control, which periodically optimizes certain variables, the energy balance has been discretized over a certain sample time, T_S.

$$E(k+1) = E(k) + T_S(P_{in}(k) - P_{out}(k))$$

3.3.1 Electrical balance

Following figure 3.10, the balance is as follows:

$$E_{bat}(k+1) = E_{bat}(k) + T_S[(\mu_{conv}V_{fc}(k)I_{fc}(k) + W_{grid_{in}}(k)) - (W_{ed}(k) + W_{tra}(k) + W_{grid_{out}}(k))]$$

with μ_{conv} the efficiency of the fuel cell's converter, V_{fc} and I_{fc} the voltage and current of the fuel cell respectively. W_{ed} corresponds to the electrical demand, in watts, W_{tra} to the electrical power that circulates through the resistance placed in the accumulator and $W_{grid_{in}}$ and $W_{grid_{out}}$ to the connection between the electrical grid and the external one, being the input and outout of power respectively.

The state of charge of the battery has a direct relation with the energy stored, only needing its Amps per Hour and nominal voltage, which can be used to avoid the aforementioned numerical problems:

$$E_{bat}(k) = 36V_{nom}AhSoC(k),$$

with V_{nom}, Ah and $SoC(k)$ the battery's nominal voltage, amps per hour and state of charge at sample time k, in %, respectively. A 3600 is needed to change from hours to seconds and dividing it by 100, as the state of charge is expressed as a percent, results in the 36. The final electrical balance is:

$$\begin{aligned} SoC_{bat}(k+1) = SoC_{bat}(k) + \frac{T_S}{36V_{nom}Ah}[(\mu_{conv}V_{fc}(k)I_{fc}(k) + W_{grid_{in}}(k)) \\ - (W_{ed}(k) + W_{tra}(k) + W_{grid_{out}}(k))]. \end{aligned}$$

3.3.2 Thermal balance

On the other hand, the thermal part is made of the fuel cell, the exchanger and the heat accumulator, as well as the different power inputs:

$$\begin{aligned} E_{accum}(k+1) = E_{accum}(k) + T_S[(\mu_{exch}(V_q - V_{fc}(k))I_{fc}(k) + \mu_{tra}W_{tra}(k)) \\ - (W_{td}(k) + W_{accum_{out}}(k) + W_{convec}(k))] \end{aligned}$$

with V_q, the fuel cell's chemical voltage and μ_{exch} and μ_{tra}, the efficiency of the exchanger and accumulator's power transfer respectively. W_{td} is the thermal demand, $W_{Accum_{out}}$ the power lost by the outputting of hot water outside the tank and W_{convec}, the power lost to the atmosphere by convection.

W_{convec} can be substituted by (3.2) but as the stored energy is a function of the temperature, (3.3), it will change to (3.4):

$$W_{convec} = h_{env}A(T_{accum} - T_{env}), \tag{3.2}$$

$$E_{accum} = m_{dip}C_{H_2O}T_{accum}, \tag{3.3}$$

$$W_{convec} = h_{env}A(\frac{E_{accum}}{m_{dip}C_{H_2O}} - T_{env}), \tag{3.4}$$

where h_{env} is the convection coefficient of the accumulator, A its convection area and T_{env}, the temperature of the environment. Also, m_{dip} is the mass of water in the tank and C_{H2O}, its heat capacity. Based on the thesis [19], the convection constant value has been set to $h_{env}A = 10W/K$. Rearranging some terms, the balance changes to:

$$\begin{aligned} E_{accum}(k+1) = (1 - \frac{h_{env}AT_S}{m_{dip}C_{H_2O}})E_{accum}(k) + T_S[(\mu_{exch}(V_q - V_{fc}(k))I_{fc}(k) \\ + \mu_{tra}W_{tra}(k)) - (W_{td}(k) + W_{accum_{out}}(k))] \end{aligned} \tag{3.5}$$

Same as before, the stored energy has been changed to a more suitable variable, the temperature, and by substituting (3.3) in (3.5), the balance has been changed to (3.6).

$$\begin{aligned} T_{accum}(k+1) = (1 - \frac{h_{env}AT_S}{m_{dip}C_{H_2O}})T_{accum}(k) + \frac{T_S}{m_{dip}C_{H_2O}}[(\mu_{exch}(V_q - V_{fc}(k))I_{fc}(k) \\ + \mu_{tra}W_{tra}(k)) - (W_{td}(k) + W_{accum_{out}}(k))] \end{aligned} \tag{3.6}$$

3.3.3 State Space system

From the two previous balances, a discrete state space representation can be computed. From the equations, it can be seen that the system will have a total of 5 inputs (fuel cell intensity, the electrical to thermal transfer resistance and the 3 security elements) along with 2 perturbations, the demands.

$$x(k+1) = Ax(k) + T_s(Bu(k))$$

$$A = \begin{bmatrix} 1 & 0 \\ 0 & 1 - \frac{k_{env}T_s}{m_{dip}C_{H_2O}} \end{bmatrix}$$

$$B = \begin{bmatrix} \frac{1}{36AhV_{nom}} & 0 \\ 0 & \frac{1}{m_{dip}C_{H2O}} \end{bmatrix} \begin{bmatrix} \mu_{conv}V_{fc} & -1 & 1 & -1 & 0 & -1 & 0 \\ \mu_{exch}(V_q - V_{fc}) & \mu_{tra} & 0 & 0 & -1 & 0 & -1 \end{bmatrix}$$

$$u = \begin{bmatrix} I_{fc} \\ W_{tra} \\ W_{grid_{in}} \\ W_{grid_{out}} \\ W_{accum_{out}} \\ W_{d_{elec}} \\ W_{d_{therm}} - h_{env}AT_{env} \end{bmatrix} \tag{3.7}$$

As an important remark, all of the parameters in both A and B have been modelled as constant, being the only exception V_{fc}, the voltage of the fuel cell, which is a function of its intensity, I_{fc}.

Chapter 4

Demand and dimensioning of the elements

Knowing the different elements that will be part of the system, the next step is to correctly size them. To do so, a look at the electrical and thermal demands used will be taken first, as it is the most important variable, being the only part of the system that consumes the generated power.

4.1 Demand

As part of the MICAPEM project, a demand was provided, which had been experimentally taken from a house located in Valencia. However, the temperature there tends to be high enough to not use the heating during most of the months, which significantly drops the thermal demand. As the aim of this master's thesis is to check the behaviour of the system when working in cogeneration, the demands will be altered at will.

Figures 4.1 and 4.2 show examples for February and August. These demands were given as samples, with a period of 15 minutes. If needed, a linear interpolation will be done.

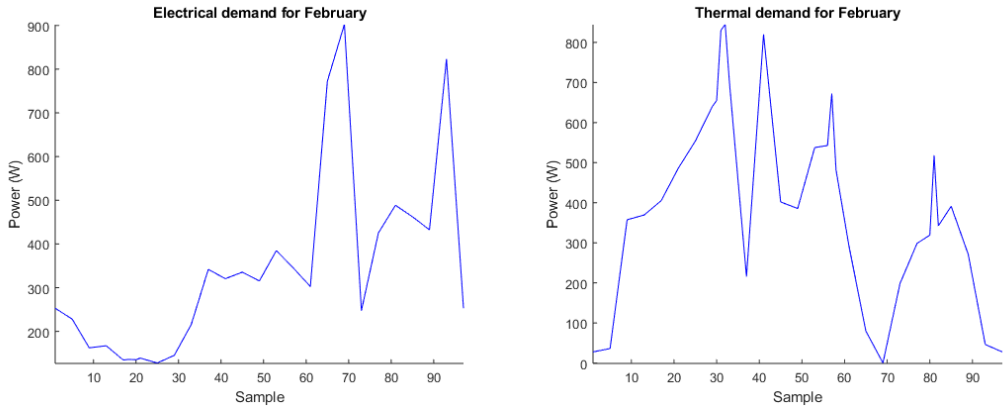

Figure 4.1: Electrical and thermal demand of February.

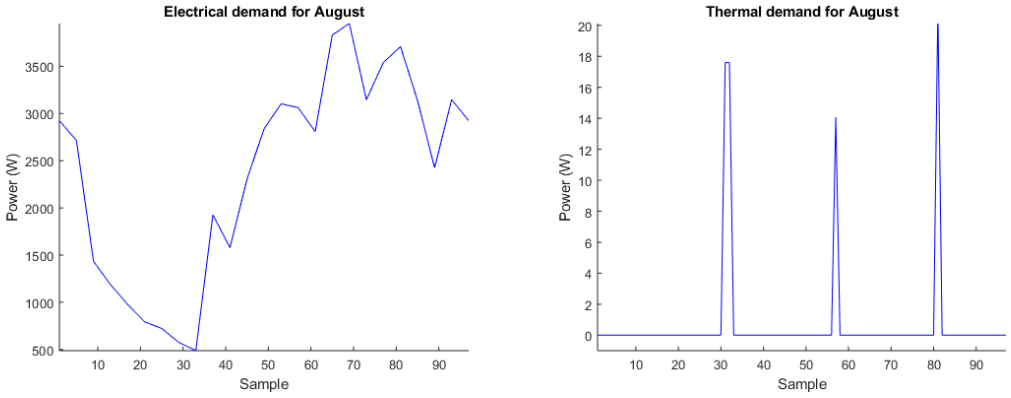

Figure 4.2: Electrical and thermal demand of August.

4.2 Dimensioning

When dimensioning the different elements of the system, the methodology used is highly dependent on the type of system, the element itself and the difference between the characteristics that these elements in the market offer.

For example, when designing an electric car, the batteries should be as large as possible, as one of the objectives is to increase their autonomy. However, this translates into more weight, increasing the energy consumed and therefore, reducing the autonomy. In this cases, a fine tuning is needed.

In other applications, the weight of the batteries isn't important, as they won't be placed in mobile parts, only having to care about its capacity, simplifying the problem.

As the aim of this project is to test how does the MPC control behave in different situations, the dimensions of the elements have been reduced enough so that the controller is forced to react to different situations.

4.2.1 Fuel cell

The first element that needs to be sized is the fuel cell. Depending on the maximum power that it can provide, the controller will hugely vary, as if it is low, the fuel cell will need to start accumulating energy sooner than another one with higher power.

While the demand is bound to have certain high peaks, the use of storing elements is due to, in part, cope with such situations. Therefore, when sizing the fuel cell, the main variable that has to be taken into account is the mean of the demand for the different months, as it will also dictate the mean of the power produced by the cell. Figure 4.3 graphically shows the mean of the two demands for all the months of the year.

Additionally, experimental data of the fuel cell Horizon3000 was available, which has a maximum electrical power of 3000 W. This is a little above the maximum mean, in July, making it a perfect candidate of a fuel cell, being used for the simulations explained later on. Figure 4.4

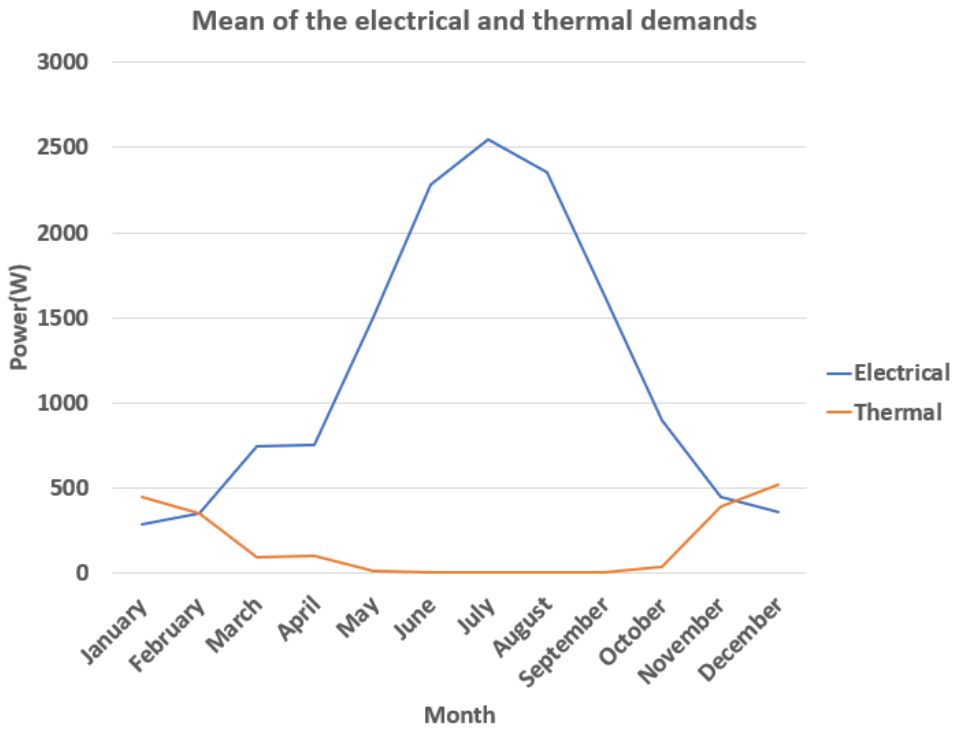

Figure 4.3: Mean of both demands for the different months.

shows the polarization curve and electrical power of the Horizon3000.

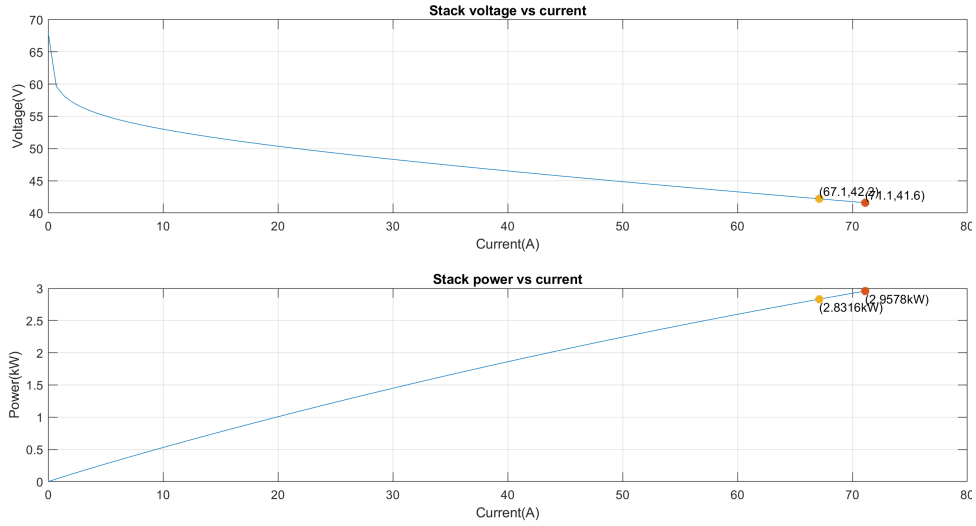

Figure 4.4: Polarization curve, at the top, and electrical power, at the bottom, of the Horizon3000.

In parallel to this master's thesis, a group of the MICAPEM project was also working in the design of a PEMFC. Close to the end of this master's thesis, its polarization curve was provided but as no time was available, it wasn't used in the simulations. Section 7.19 will show the possible changes that these might suffer when using this fuel cell.

4.2.2 Battery

In the case of the battery, there is a huge variety to pick from, varying both in parameters as well as price. Additionally, there is another layer of freedom as they can be stacked in parallel, increasing its total voltage or in series, changing instead the rated capacity.

As most of the batteries available are good enough for this project, the battery shown in figure 4.5 has been used, which was an already available one.

Figure 4.5: Battery used in the simulation.

In general, when coupling batteries together, they are put some in parallel and some in series, increasing the overall voltage and rated capacity. The final stack of batteries used had a total of 10 in parallel and another 8 in series, resulting in the battery parameters being:

Parameter	Value
Nomival voltage (V)	32
Rated Capacity (Ah)	160

Table 4.1: Parameters of the battery.

4.2.3 Heat accumulator

In the case of the water tank, the only parameter that can be dimensioned is the amount of liters stored. if this is too high, the thermal dynamics will be, in general, ignored, as the temperature of the water won't vary enough to reach its limits. To make it so that this isn't the case, the liters in the tank have been set to 200 L, large enough to store enough thermal energy but low enough to force the MPC to interact with its limits.

It is worth mentioning that the tank used must physically be able to insert and extract water from the exterior, as, specially in the summer months, the water inside the accumulator will have to be refreshed periodically or it will boil. Figure 4.6 shows a possible candidate of a water tank that meets this conditions.

Figure 4.6: Example of a water tank [20].

4.2.4 Transfer resistance and security elements

Lastly, for the rest of the elements, they can be dimensioned much more freely. In the case of the electrical to thermal element, the resistance can hugely vary, as well as the intensity that runs through it. As for the security elements, the amount of thermal power extracted will be controlled via a valve and the electrical power via converters. These can also vary in size, according to the needs of the system.

Due to physical constraints, the minimum values were all set to zeros and for the maximum ones, they can be seen in the following table:

Elements	Minimum power (W)	Maximum power (W)
Transfer resistance	0	1000
External grid converter	0	1000
Water tank valve	0	4000

Table 4.2: Limits of the transfer resistance and security elements.

Chapter 5

Model Predictive Control (MPC)

Having modelled the system with Simulink, the next step is to create the controller that will decide what intensity will be given to the fuel cell. For this application, a Model Predictive Control (MPC) has been implemented.

From section 5.8, it can be seen that the demand is a huge factor in the development of the system, as it is almost exclusively the only factor of power consumption. It has two properties that make the MPC control, the more suitable one. First of all, the demand from one day to the next tends to be very similar, as the environmental conditions haven't substantially changed, making it a periodic perturbation, which helps with its modelling.

Additionally, the demand also has big spikes, which correspond to elements such as showers, dishwasher or the use of the kitchen's electrical appliances. By using a predictive controller, it will preemptively start storing energy in the battery and heat accumulator for when the big spikes arrive. Without this prediction, the system might be unable to generate enough power.

Moreover, an MPC control is able to handle multiple-input multiple-output systems (MIMO) that have interactions between their inputs and outputs, seen by the state space matrices in 3.3.3. As it is a multivariable controller, it can control all the outputs simultaneously.

Additionally, when it comes to the fuel cell, and the use of hydrogen, the objective isn't only to find a solution that will keep the demand supplied at all times, but rather to do so while minimizing the hydrogen consumed. This is further complicated by the fact that the system has a set of constraints which cannot be broken as, for example, charging an already full battery would rapidly break it. This can be easily done using an MPC, which already takes into account all of this limits when deciding the best suitable control.

5.1 Theoretical background

As the name itself indicates, the Model Predictive Control bases its control strategy in the prediction of how the system will evolve in the future. It is mainly divided into two parts, the first one being the model of the system, and the second one, the optimizer.

By using the model, the controller is capable of knowing what will happen in the future, being better the more accurate the model is. With the optimizer, it will be able to decide what are the optimal inputs that will minimize an objective function, such as the consumed hydrogen. This prediction is limited to a fixed number of sample times in the future, called prediction horizon.

For example, taking a look at figure 5.1, the system is at time k. At the left side of time k, the past is represented, where the already implemented inputs of the system and the sensored outputs can be seen. At the right side, the predicted future is shown and for this case, a prediction horizon of size p has been used.

The objective in that figure is the tracking of the reference trajectory, therefore ideally, at the end of the prediction, the predicted output of the system will be at such reference. In other words, the objective function to minimize is the sum of all the errors between the predicted output and the reference points throughout all the trajectory, which will be done by the optimizer. The control actions to achieve such results are seen in teal in the figure.

Lastly, and in order to ensure that the system keeps evolving to the desired states, only the inputs predicted for the first sample time are applied. This is because the model will most likely not be a perfect representation of the real system, and along with some possible disturbances the system might have, the next inputs might have to change. In the next iteration, the sensors will read the state of the system and start another prediction, followed by the optimization.

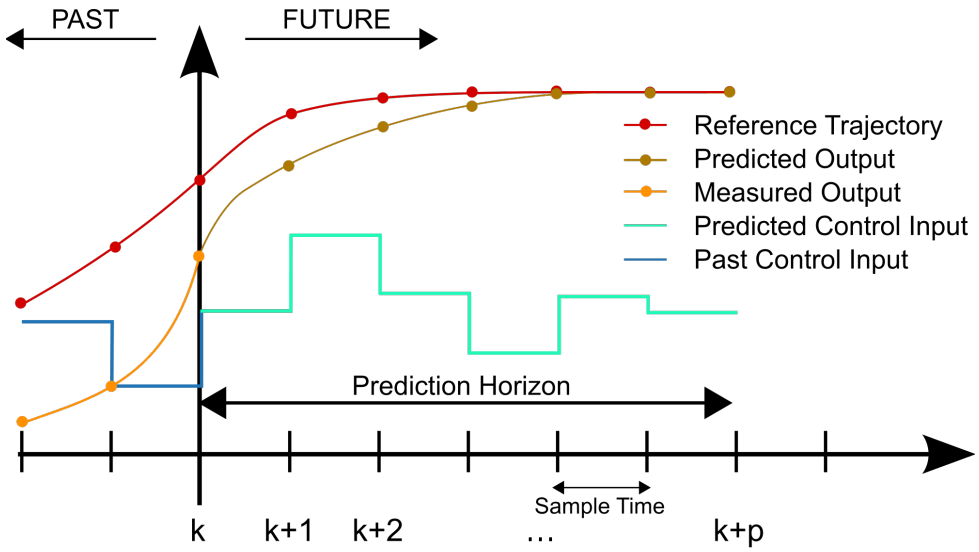

Figure 5.1: Graphical representation of an MPC [21].

Another very important part of the MPC is the capability of implementing constraints into the system. As the decision process is done via optimization, the addition of constraints into the problem can be easily done, such as limiting the intensity that passes through a sensitive electrical element or the acceleration of an occupied vehicle, which has to be capped at a value to avoid damaging the occupants.

5.2 Designed controller

5.2.1 Objective function

While the objective is to supply power to the electrical and thermal demands, the controller should do so utilizing the minimum amount of hydrogen possible, and therefore, its cost. Additionally, as seen in (3.1), the relationship between the hydrogen flow and the fuel cell's intensity is directly proportional. Therefore, one of the variables to minimize in the objective function has been the intensity run through the fuel cell.

Moreover, with the aim of reducing the energy used, the cell's intensity isn't the only input, as when the battery is at low charge, power can also be taken from the external grid, having to be minimized as well. That also applied to the other two security elements, the battery discharging energy into the external grid and the accumulator's exchange of hot water with cold one. While this isn't exactly a reduction in energy production, as it has already been produced, it is wasted energy, which perhaps a better controlled wouldn't have generated in the first place.

Additionally, when dealing with batteries, discharging the battery down to almost zero percent causes them to degenerate in the long run, and the same happens if they are charged up to one-hundred percent, specially for Li-ion batteries. To avoid this, soft constraints have been added which, contrary to the hard ones, can be bypassed. This is done by adding to the hard constraints a variable that widens their range, and in order to ensure that this is only done when needed, such variable is also minimized in the objective function.

Lastly, when using an MPC, a curious behaviour is seen in the inputs, where its optimal behaviour tends to be either its minimum value, when no energy is needed, and its maximum one when, on the contrary, energy must be produced. Obviously, this should be avoided and to do so, their derivatives must also be minimized. Taking for example the intensity of the fuel cell, figure 5.2 shows the results of a simulation with this behaviour, where each iteration corresponds to a control action, done every 15 minutes.

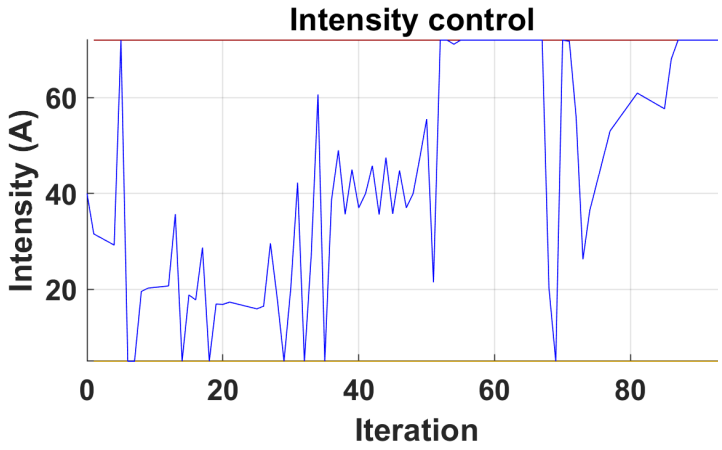

Figure 5.2: Behaviour of the fuel cell's intensity without the minimization of its derivative.

5.2.2 Constraints

About the constraints of the system, it is important to remember that the objective is to predict the behaviour of the system, therefore its model must be present in the constraints. Also, the initial state space variables have to be fixed to the values of the system sensored in that moment.

On the other hand, the next constraints are the maximum and minimum values of energy that the battery and accumulator can store. While in the case of the battery these limitations are physical ones, as it cannot hold either negative energy or more than its fully charged point, the accumulator ones aren't, having been set such that the water's temperature is neither too cold to be able to supply heat nor too hot to transform into steam.

Furthermore, all the system inputs also have to be constrained between a minimum and maximum value, as they all have physical limitation, being the minimum one zero, as they are one-directional. As the demands are also considered inputs, additional constraints have to be set, that force the variables that model them to a set value, as it isn't possible to change them.

The last constraints are the soft ones and the mathematical expressions that ensure the security elements aren't always activate. These last one will be explained in the next chapter, as they are based on mathematical equations.

5.2.3 Mathematical formulation and numerical numbers

With the objective and constraints known, they now have to be expressed in mathematical format so that the optimizer will be able to understand them.

For the objectives, the problem is a multiple optimization one, being each one of the following objective function an optimization problem on its own, with k equal to the simulation iteration and H_p the prediction horizon:

$$J_1(k) = \sum_{i=0}^{H_p} ||I_{fc}(k+i)||_1$$

$$J_2(k) = \sum_{i=0}^{H_p} ||e(k+i)||_1$$

$$J_3(k) = \sum_{i=0}^{H_p} ||W_{grid_{in}}(k+i)||_1$$

$$J_4(k) = \sum_{i=0}^{H_p} ||W_{grid_{out}}(k+i)||_1$$

$$J_5(k) = \sum_{i=0}^{H_p} ||W_{accum_{out}}(k+i)||_1$$

where $J_1(k)$ is the fuel cell's current function with $I_{fc}(k+i)$, the current produced by the fuel cell at simulation time k+i. $J_2(k)$ corresponds to the soft constraints' and $e(k+i)$, the variables that restrains the soft constraints, see (5.10). $J_3(k)$ and $J_4(k)$ are the functions of the security elements of the battery and $J_5(k)$, the accumulator ones. $W_{grid_{in}}(k+i)$, $W_{grid_{out}}(k+i)$ and $W_{accum_{out}}(k+i)$ are the power of the security elements. $||x||_1$ refers to the 1-norm of x.

For the derivatives, the mathematical expressions can be seen in (5.1) to (5.5). It is important to additionally minimize the difference between the first inputs and their sensored values, shown as the variables with the subindex , pre.

$$J_6(k) = \sum_{i=2}^{H_p} ||I_{fc}(k+i) - I_{fc}(k+i-1)||_1 + ||I_{fc}(1) - I_{fc,pre}||_1 \tag{5.1}$$

$$J_7(k) = \sum_{i=2}^{H_p} ||W_{tra}(k+i) - W_{tra}(k+i-1)|| + ||W_{tra}(1) - W_{tra,pre}||_1 \tag{5.2}$$

$$J_8(k) = \sum_{i=2}^{H_p} ||W_{grid_{in}}(k+i) - W_{grid_{in}}(k+i-1)||_1 + ||W_{grid_{in}}(1) - W_{grid_{in},pre}||_1 \tag{5.3}$$

$$J_9(k) = \sum_{i=2}^{H_p} ||W_{grid_{out}}(k+i) - W_{grid_{out}}(k+i-1)||_1 + ||W_{grid_{out}}(1) - W_{grid_{out},pre}||_1 \tag{5.4}$$

$$J_{10}(k) = \sum_{i=2}^{H_p} ||W_{accum_{out}}(k+i) - W_{accum_{out}}(k+i-1)||_1 + ||W_{accum_{out}}(1) - W_{accum_{out},pre}||_1 \tag{5.5}$$

where, from $J_6(k)$ to $J_{10}(k)$, correspond to the fuel cell's intensity, transfer resistance, and security elements, respectively.

Therefore, the objective function to be minimized will be the sum of all the ones explained above, (5.6). However, by only summing them up, the controller will focus on the minimization of the variable with higher magnitude. To avoid this, the variables have to be divided by their maximum value, making their range between zero and one.

Additionally, not all the variables are of the same importance in the system. For example, while minimizing the derivative of the control variables is important, the minimization of the variables themselves is much more desired. Therefore, weights have to be added, which will make the controller minimize the ones with a higher one.

$$J(k) = \sum_{i=1}^{9} w_i \frac{J_i(k)}{\bar{u}_i}, \tag{5.6}$$

with w_i the weight of the variable and $\bar{u}$, their maximum values, seen in table 5.2. The weights will be decided in section 5.3 and as names will be given to the different weights and maximum values, the objective function (5.6) will change to:

$$J(k) = W_{fc}\frac{J_1(k)}{I_{fc,\,max}} + W_{sc}J_2(k) + W_{se}(\frac{J_3(k)}{W_{grid_{in},max}} + \frac{J_4(k)}{W_{grid_{out},max}} + \frac{J_5(k)}{W_{accum_{out},max}}) \\ + W_{dfc}\frac{J_6(k)}{I_{fc,\,max}} + W_{dtra}\frac{J_7(k)}{W_{tra,\,max}} + W_{dse}(\frac{J_8(k)}{W_{grid_{in},max}} + \frac{J_9(k)}{W_{grid_{out},max}} + \frac{J_{10}(k)}{W_{accum_{out},max}}). \tag{5.7}$$

In the case of the constraints, the ones related to the model can be seen in (5.8) and (5.9), the last one being the equality between the first state space variables and the sensored ones, where $k = 1, \ldots, H_p$.

$$x(k+1) = Ax(k) + Bu(k) \tag{5.8}$$

$$x(1) = x_{pre} \tag{5.9}$$

Additionally, (5.10) shows the equations needed in order to create the soft constraints of the battery.

$$SoC_{lsc}(k)(1-e(k)) + SoC_{min}(k)e(k) <= SoC(k) <= SoC_{hsc}(k)(1-e(k)) + SoC_{max}(k)e(k)$$

$$0 <= e(k) <= 1, \tag{5.10}$$

where SoC_{lsc} and SoC_{hsc} are the low and high values of the soft constraints. With e equal to 0, only the soft constraint values will remain, forcing the state of charge to be between the two. On the contrary, if e is equal to 1, the soft constraints term will cancel out and the SoC will now be limited between its minimum and maximum values.

For the accumulator, only hard constraints are needed:

$$T_{min}(k) <= T(k) <= T_{max}(k), \tag{5.11}$$

being $T_{min}(k)$ and $T_{max}(k)$ the minimum and maximum value of the temperature. Moreover, all the inputs are also bounded between a predefined minimum and maximum value:

$$I_{fc,min}(k) <= I_{fc}(k) <= I_{fc,max}(k)$$

$$W_{tra,min}(k) <= W_{tra}(k) <= W_{tra,max}(k)$$

$$W_{grid_{in},min}(k) <= W_{grid_{in}}(k) <= W_{grid_{in},max}(k)$$

$$W_{grid_{out},min}(k) <= W_{grid_{out}}(k) <= W_{grid_{out},max}(k)$$

$$W_{accum_{out},min}(k) <= W_{accum_{out}}(k) <= W_{accum_{out},max}(k)$$

Additionally, in order to ensure that the security elements are only active when it is wanted, a set of equations have to be set. (5.12) and (5.13) are an example for the entrance of power from

the external grid into the system. $y(k)$ is a binary variable that, when set as 0, prevents the input from activating, as seen in (5.13). (5.12) is the responsible of forcing the binary variable to 0 when the state of charge is above a set value.

$$y(k) <= \frac{(SoC_{lsc}(k) - SoC(k))}{SoC_{max}} + 1 \tag{5.12}$$

$$W_{grid_{in}}(k) <= y(k) W_{grid_{in},max}(k) \tag{5.13}$$

Lastly, the table 5.1 shows the values used for the constraints of the state space variables and table 5.2, for the input ones. For this last table, the decision of minimum and mximum values of the power are the same ones as in section 4.2.4.

Parameters	Values	Parameters	Value
SoC_{min}	10 %	SoC_{max}	100 %
SoC_{lsc}	20 %	SoC_{hsc}	90 %
T_{min}	65 ºC	T_{max}	95 ºC

Table 5.1: Limits of the system inputs.

Parameters	Values	Parameters	Value
$I_{fc,min}$	10 A	$I_{fc,max}$	72 A
$W_{tra,min}$	0 W	$W_{tra,max}$	1000 W
$W_{grid_{in},min}$	0 W	$W_{grid_{in},max}$	1000 W
$W_{grid_{out},max}$	0 W	$W_{grid_{out},min}$	1000 W
$W_{accum_{out},max}$	0 W	$W_{accum_{out},min}$	4000 W

Table 5.2: Limits of the system varaibles.

5.3 Parametrization of the objective's weights

5.3.1 Pareto Front

When deciding which weights will be used, a good approach is to start with a simplified version of the system that doesn't include all the control variable, and after the weights of this simplified version have been set, expand it until the desired system's weights are set.

In the case of this system, the simplest model one can achieve is when all the inputs but the fuel cell are deactivated and the derivatives, ignored. This leaves the multiple optimization problem into a bi-dimensional one, having only the fuel cell's intensity and the soft constraints weights left.

While technically there are two soft constraints, their weights have been supposed equal, as none is more important than the other. This has also been applied to the security elements. If this wasn't the case, then further simplifications should be taken, as the amount weights would have increased,

Remarking the fact that it is common practice to set the sum of all weights to 1, it can be seen that for the bi-dimensional problem, only one parameter is needed. For this cases, a Pareto front can be used [22, 23], a graphical representation of the changes of the objective function when the two weights vary.

To do so, the same simulation has to be run multiple times, where the only changes between them are the values of the weights. From these simulations, the total objective function has to be calculated, and the weights of the smaller objective value, are the ones chosen.

It is important to run this optimization throughout all the simulation. In cases where the behavior of the system hugely varies between simulations, several Pareto fronts should be done, resulting in more than one set of weights for the optimization. Figure 5.3 shows the Pareto front of the system.

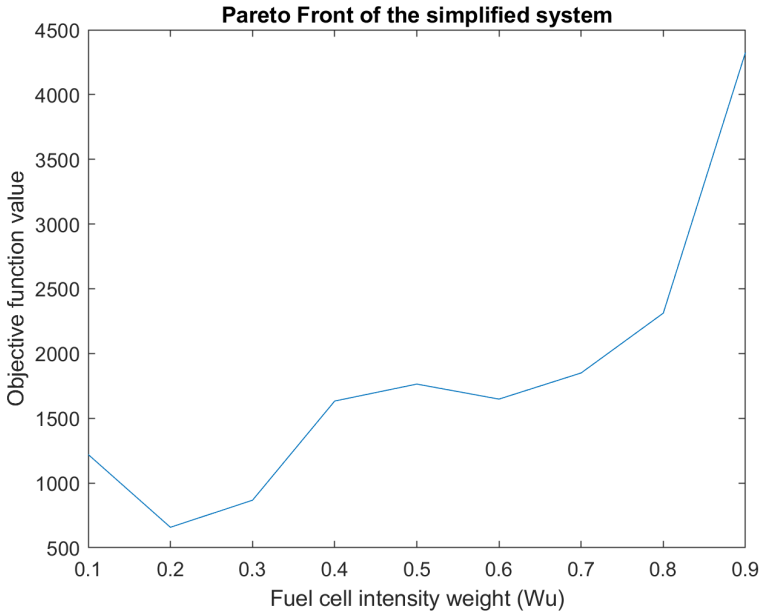

Figure 5.3: Pareto front of the simplified system.

Which results in the following weights, where the $-$ symbol represent still unset ones:

Variable type	Weight	Value
Input	Fuel cell's I (W_{fc})	0.2
	Soft constraints (W_{sc})	0.4
	Security elements (W_{se})	-
Derivative	Fuel cell's I (W_{dfc})	-
	Transfer resistance (W_{dtra})	-
	Security elements (W_{se})	-

Table 5.3: Weights of the objective function 5.7

5.3.2 Soft constraints and security element

The next step is to decide the values that the weights of the security elements will have. In this case, a Pareto front could have also been applied, changing from a 2D function as seen in the previous section to a 3D or 4D one, depending on the methodology. However, the important aspect in this part isn't the value of the weights themselves, but whether or not they are higher or lower than the soft constraints ones.

Let's suppose that the battery reaches the lower soft constraint and that the intensity of the fuel cell is already at the maximum value. In this situation, power can only be drawn from either the battery, unsatisfying the soft constraints, or from the external grid. As the objective is to minimize, the optimizer will decide that the best approach is to take the energy from the one with the lower weight. This can also be applied to the other 2 security elements, being the behaviour identical.

As discharging the battery below the soft constraints point is much less costly than drawing power from the grid, and the extraction of hot water should also be avoided, it was decided that W_{sc} should be lower than W_{se}. After some trials, the weights changed to:

Variable type	Weight	Value
Input	Fuel cell's I (W_{fc})	0.08
	Soft constraints (W_{sc})	0.16
	Security elements (W_{se})	0.20
Derivative	Fuel cell's I (W_{dfc})	-
	Transfer resistance (W_{dtra})	-
	Security elements (W_{se})	-

Table 5.4: Updated weights of the objective function 5.7

5.3.3 Derivatives

Lastly, the weight of the derivatives must also be set. In this case, the desired weights have to be higher than zero, but not high enough that it will make the system stop from changing when needed. Again, after some testing, the derivatives were set 0.005, satisfying the desired behaviour. Therefore, the other weights have changed to:

Variable type	Weight	Value
Input	Fuel cell's I (W_{fc})	0.078
	Soft constraints (W_{sc})	0.156
	Security elements (W_{se})	0.195
Derivative	Fuel cell's I (W_{dfc})	0.005
	Transfer resistance (W_{dtra})	0.005
	Security elements (W_{se})	0.005

Table 5.5: Updated weights of the objective function 5.7

Chapter 6

Implementation of the controller

After creating the controller, the next step was to implement it. To do so, Yamlip was used, a modelling and optimization toolbox that allows the creation of problems at a high-level programming language. Additionally, this can also be installed as a Matlab toolbox, which greatly facilitates the creation of the optimizer.

Yalmip however, doesn't incorporate a solver, so one must be chosen. The optimization problem can be as complicated as wanted, but seeing that the model of the system is almost linear, a linear optimization should be good enough for the MPC to predict the future behaviour. Therefore, a linear solver should be picked. Of all the possibilities Mosek is a good candidate, as it is free for academia. Most of these linear solvers can also solve mixed integer one's, in case integer or binary variables are needed, Mosek included.

6.1 Simulation algorithm

To run the controller on the system, a script was made with the following procedure, which can be seen in Algorithm 1. First of all, the parameters of the system are initialized, as well as its initial states and inputs. Additionally, the MPC parameters also need to be defined, which are, among others, the sampling time T_S and the prediction horizon H_P.

The MPC demand is then selected, which is read from an Excel file. In order to generate the real demand, a function was made that allowed its customization. Starting from the modelled demand, a series of changed could be done. First of all, a random components could be added meant to simulate a mismatch between the modelled demand and the real one, which is bound to happen in the real implementation. This, however, didn't change the mean of the real demand. Therefore, a flat number could be added or subtracted to this demand to test different scenarios.

Next, and highly dependent on the demand, the length of the simulation was defined. A plot of the initial states and inputs was also done, which will be updated later on.

With the initialization finished, a loop was created, that run the simulation. At the start of every

iteration, the inputs of the system were calculated with the MPC. The Simulink simulation was then run for a duration equal to the sample time, and using the previous calculated inputs. The final states of the simulation were saved, as they will be used in the next iteration, as well as stored and plotted.

Algorithm 1 Algorithm used for the simulations

Data: System and MPC parameters, states x_{k-1} and inputs u_{k-1}
Results: d_{mpc}, d_{real}, x_t, u_t

Generate the real demand, d_{real}, and the MPC's expected one, d_{mpc}
Set the simulation length k_{max}
Plot the initial states and inputs

while k is smaller than k_{max} **do**
    Get u_k from the MPC
    Simulate the system for T_S ▷ with T_S the sampling time
    Save the states x_k
    Store x_k and u_k in x_t and u_t
    Set x_{k-1} equal to x_k and u_{k-1} to u_k ▷ Prepare for next iteration

    Update the plot
    Print information about the iteration
end while
Print some information of the simulation

Some information was also printed at the end of the each iteration, seen in figure 6.1, being whether or not the MPC achieved a feasible solution (seen as "Done!" if it was), along with the computing time of all the simulation.

```
For i = 1/97: Done!         t = 36
For i = 2/97: Done!         t = 81
For i = 3/97: Done!         t = 92
For i = 4/97: Done!         t = 103
For i = 5/97: Done!         t = 114
For i = 6/97: Done!         t = 123
For i = 7/97: Done!         t = 133
For i = 8/97: Done!         t = 142
For i = 9/97: Done!         t = 152
For i = 10/97: Done!         t = 162
For i = 11/97: Done!         t = 171
For i = 12/97: Done!         t = 181
For i = 13/97: Done!         t = 190
For i = 14/97: Done!         t = 200
For i = 15/97: Done!         t = 210
```

Figure 6.1: Information displayed every iteration.

Figure 6.2 also shows the information that the script showed when the simulation finished. This was all related to the time taken to finish the simulation, being the total time spent, the time used to optimize, simulate and plot, as well as the time per iteration.

```
Total time spent:   1085.7675 seconds
-> Time optimizing: 973.4028 seconds (89.6511%)
-> Time simulating: 37.6325 seconds (3.466%)
-> Time plotting:   20.7874 seconds (1.9145%)
Time per iteration: 11.1935 seconds
```

Figure 6.2: Information displayed at the end of the simulation.

6.2 MPC algorithm

With the use of Yalmip, the MPC implementation was straightforward, and it can be seen in Algorithm 2. First of all, the model was defined, which meant the creation of the matrices A and B, as they will be used in the constraints. The next step was to create the optimization variables and with them, both the objective function and the constraints.

Here is where Yalmip helpfulness was seen, as these three components could be treated as normal Matlab variables. For example, when defining the objective function, a loop was done between 1 and the prediction horizon, and in each iteration, the new functions could be quickly incorporated by adding them to the existing one. A similar behaviour could be used with the constraints. With the problem set up, the last step needed was to solve it.

Algorithm 2 First MPC

Data: Previous states x_{k-1} and inputs u_{k-1}
Results: Controlled input u_k

1: Compute model matrices A and B
2: Set the optimization variables
3: Set the objectives and constraints
4: Solve the optimization problem

However, from a computation point of view, this algorithm is extremely inefficient, as the optimization problem is being set in each iteration, where in reality, it has very little change from one to the next. Therefore, algorithm 2 was changed to algorithm 3.

The main difference was that the optimization problem was only created in the first iteration, and the variables, set to *persistent* so that they weren't erased, being able to call them again in the next ones. But not all constraints were constant, and therefore, could not be created with this method.

This was the case of the perturbation variables as well as the initial states, fixed by the sensors, having to be defined in each iteration.

Algorithm 3 Implemented MPC

Data: Previous states x_{k-1} and inputs u_{k-1}
Results: Controlled input u_k

1: **if** first iteration **then**
2: Compute model matrices A and B
3: Set the optimization variables
4: Set the constant objectives and constraints
5: **end if**
6: Set the rest of the constraints ▷ Demand and states initial values
7: Solve the optimization problem

6.3 Some customization

Lastly, in order to be able to further customize the simulations, a series of variables were added to both the script and the MPC that allowed the complete shut-off of any of the complementary inputs to the fuel cell: resistance in the water tank, connections to the external grid and accumulator's hot water valve. This helped in the debugging of the script and Simulink model and allowed the simulation of a failure of one of these elements.

Chapter 7

Simulations and Results

In this chapter, the different simulations that have been done throughout the master's thesis will be explained, as well as the conclusions taken from them. It has been divided in three chapters. First of all, the use of a simplified system in order to faster debug the controller. Then, the different simulations done to set parameters such as the sampling time, the horizon prediction or the PI control. Lastly, the results of the finished controller and model will be explained.

7.1 Linear system

Before starting the simulations with the real model, it is important to note that during the first iterations of both the controller as well as the model, there will most likely be unseen errors that will cause the results to not behave as expected. This errors are very varied and in order to ensure that all of them have been corrected, a simplified version of the model has been created, highly reducing the possible number of errors of the model. Figure 7.1 shows such simplified model. In the figure, uk is the input vector and dk, the demands' one.

In this case, taking a look at the state space equations, section 3.3.3, it is seen that the only non-linear parameter is the voltage produced by the fuel cell, which according to the polarization curve, doesn't have a huge variation between low intensities and high ones. By choosing an intermediate value, and supposing that the voltage is constant and therefore independent from the intensity, the system becomes linear. Then, the system becomes much easier to model, as the state space matrices can be used.

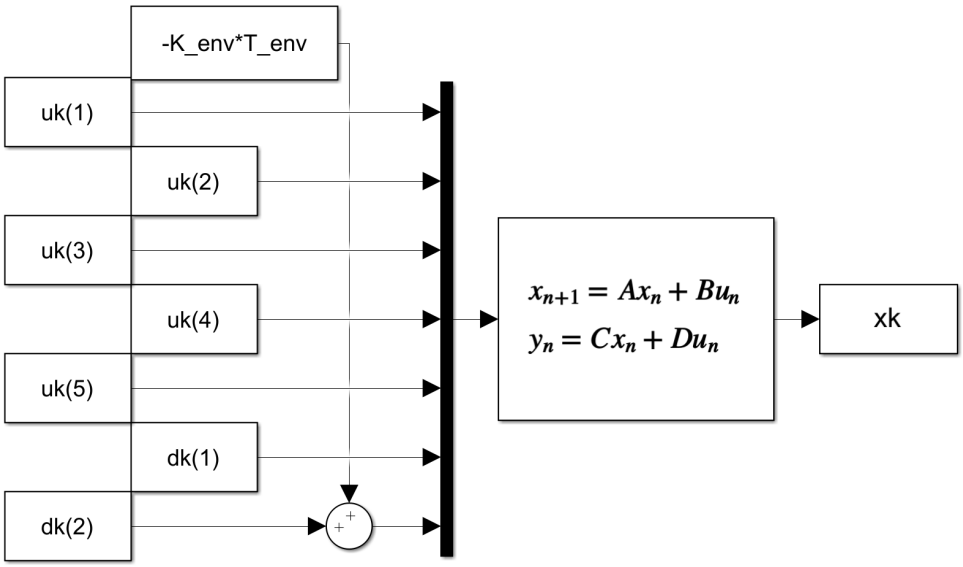

Figure 7.1: Linear system of the model.

7.2 Model comparison

After the real model was completed and all the errors debugged, it was seen that the simulations that used such model tended to last for hours, as the electrical grid had to be simulated in detail. Therefore, a more in-depth comparison between the simplified and the real one was made, to see if it was possible to use it as a reference.

First of all, a tentative test was made, which ran, in the same simulation, both models in parallel, meaning in each iteration, they both models had the same initial parameters as well as inputs. Then, the state space variables of both were compared. The maximum error was lower than 2%, concluding that both models were indeed, the same.

However, the previous test only checked the error created in each iteration, as they were both initialized to the same values every time, resulting in the accumulated error being ignored. Therefore, a second one was done, which run both models independently, having both of them the same parameters and demands. The intensity, transfer resistance and state space variables are shown in figure 7.2, having the linear model in blue and the non-linear in red.

Comparing the results, while they aren't exactly the same, specially for the transfer resistance, the general behaviour of the system can be considered as the same. For this case, as the intensity of the fuel cell was at around 30 A, the real voltage of the fuel cell was higher than the constant one used for the linear model. This resulted in the linear model supposing a lower electrical energy produced, as well as higher thermal one. This creates an accumulated error that must be supplied by the peaks in the transfer resistance. However, while both models cannot be considered equals, the linear model is similar enough to be used as a reference of its behaviour.

Additionally, as the ohmic region of the polarization curve has a very linear behaviour, if a more precise behaviour is needed, a Linear Parameter-Varying (LPV) control can be added to the MPC.

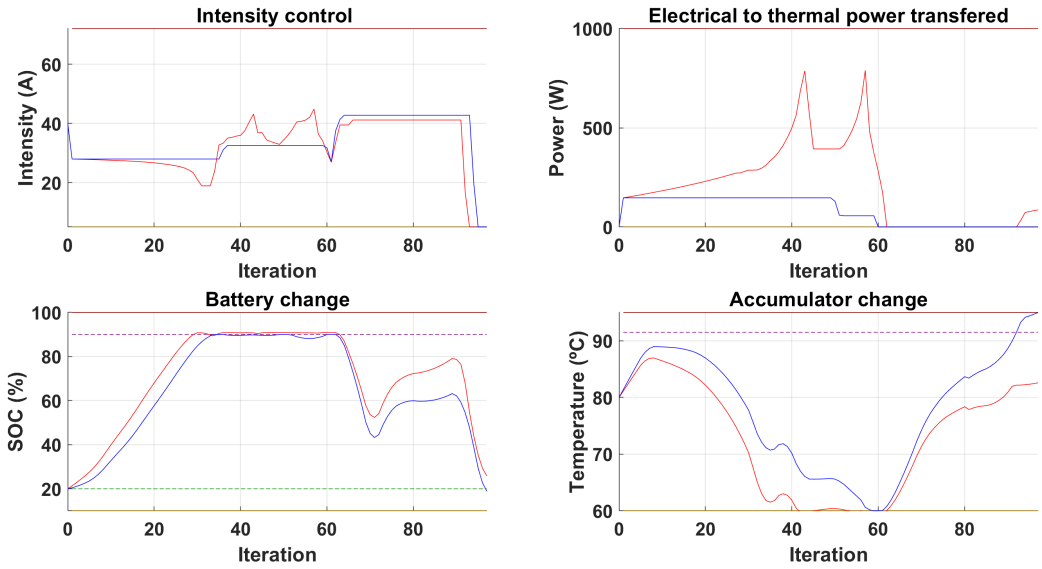

Figure 7.2: Comparison between the linear system, in blue, the non-linear one, in red.

7.3 Early simulations

After having made sure that both the controller as well as the model are correctly created, it is time to decide the values of several parameters that will affect the response of the system. All these simulations were done using the previosuly explained model, seen in chapter 3

7.3.1 Grid's PI control

The first element that has been analyzed was the PI control of the grid, due to its independence with the rest of the parameters in the system. As a remainder, the objective of the PI is to ensure that the grid's voltage is maintained at a constant value.

As the change in demand will be almost instant, for example turning on the oven, a drop in voltage is bound to happen. This cannot be completely negated but the controller has to be designed in such a way that this change in the grid's voltage is minimum, while also reaching the reference voltage in a small amount of time.

The first parameter that will be set is the sampling time. The chosen value of T_S has been equal to 1 ms, as it is the one that is used in similar applications. For both the K_P and K_I, some testing is needed, to see the effect of their changes in the response of the voltage.

With values of the proportional gain lower than 8, the controller struggled to arrive to the stationary, oscillating around the reference voltage; and for higher than 15, the response time quickly increased, with no huge change in the overshoot. Therefore, a value of $K_p = 10$ was chosen.

Additionally, for integral gains over 3, a similar behaviour happened, increasing the settling

time and the oscillations around the reference. For low enough values, the system was incapable of reaching the reference voltage. For this system, this gain was set to $K_I = 2$.

This resulted in a settling time of 20 seconds and, for an instant change in demand of 1000W, a voltage drop of 2V. The first two peaks in figure 7.3 show the behaviour of the grid's voltage for a change of 1000W and the other two, for 2000W.

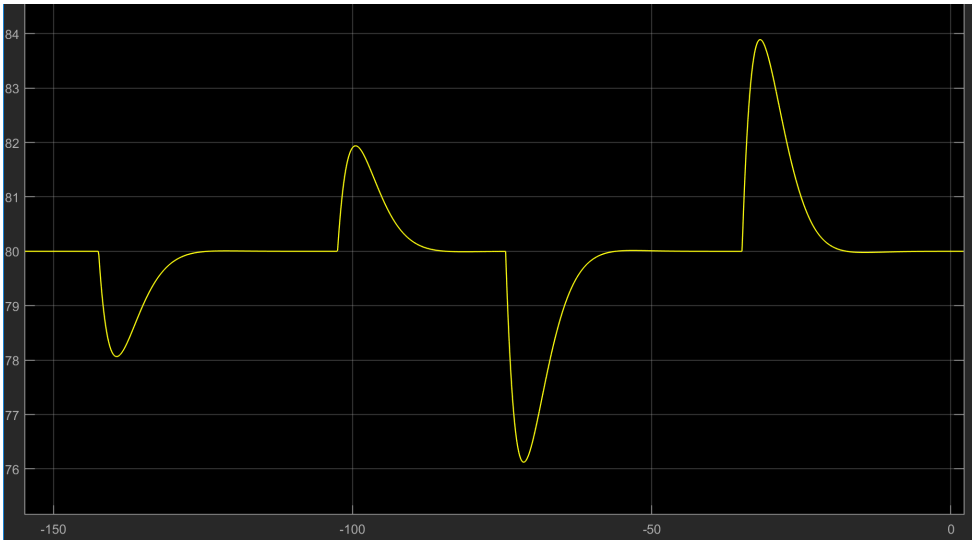

Figure 7.3: Behaviour of the grid's voltage (seen in the vertical axis) with a change in demand.

7.3.2 Sample time

Next, the sampling time has been decided. While the demand in houses can hugely vary from one time to another, this demand has been previously modelled, having it incorporated into the model of the system, meaning that such changes will be predicted. Therefore, problems will arise when the expected demand hugely varies from the real one, and only when it is across many samples, as the MPC is able to adapt to punctual cases.

These allows the sampling time to increase to values higher than 5 minutes, which tends to be the used ones for similar applications. As the modelled demand has been sampled every 15 minutes, it was decided to use this sampling time as the one at the start, and lower it later on if needed. In case of a smaller sampling time than 15 minutes, an interpolation will have to be done for the demand, as no values have been gathered. However, as it will be seen in the next section, this wasn't needed.

7.3.3 Prediction horizon

Closely related to the sampling time is the prediction horizon. For this parameter, there is a clear objective which is to make it as large as possible. By having a large value, the controller will be able to react earlier to incoming changes, creating smoother results. However, this value is limited by the computation power, as the higher the prediction horizon grows, the harder the optimization will be and the more variables it will have.

In applications where the system has a periodic behaviour, the minimum prediction horizon sought for is the value that will include such period, so that the controller takes all of it into account. This is where the sampling time comes in. Taking the value of 15 minutes, a full day equals to a prediction horizon of 97. With these parameters, a simulation with the simplified system takes about 10 minutes per day, which is a reasonable amount of time. By reducing the sampling time, the simulation time rapidly increased, while having no significant changes in the response. In the case of the simulations that involved the real model, these variations in sampling time or prediction horizon had no effect on the time as less than 5% of it was spend optimizing.

Therefore, for the simulations, a sample time of 15 minutes was used, as well as a prediction horizon of 97, corresponding to a full day.

7.4 Final Results

With the previous parameters set, the system explained in chapter 3 was then analyzed, testing the controller in different situations to ensure its correct behaviour as well as to check how it would behave in extreme situations.

7.4.1 Perfectly modelled demand

The first testing done was the most simple one, where the modelling of the demand has been done perfectly, being the real and the predicted one, equal. With this simulation, the behaviour of the system will be able to be tested without worrying about possible errors due to a demand incorrect modelling. Figure 7.4 and 7.5 show the results for February, where the demand has been multiplied by 4 to force the system to interact with the constraints. The security elements aren't shown as they haven't activated. The dashed lines in the battery correspond to the soft constraints and the limits of the activation of the security elements. For the accumulator, only to the activation of its valve.

From the results, the intensity tends to remain at around 30 and 40 A, increasing a little over time, and having some spikes between sample times 30 and 60. When the simulation starts, the intensity is set such that the battery will start storing enough energy for the peaks of demand at around iterations 68 and 93. Almost 8 hours later, at iteration 30, the effect of the soft constraints can be seen as the fuel cell produces just enough energy to not surpass the limit.

At the same time, while the temperature started at 80ºC, it rapidly fell to its minimum value of 60ºC. However, the controller has predicted this behaviour, activating the resistance inside the accumulator from the beginning, to transfer this electrical energy excess into the needed thermal one.

As the day passes by, the thermal demand decreases, and the electrical increases. For this part, the controller sets the fuel cell to a constant value in order to end up with the battery at the lowest soft constraint. This doesn't end up being exactly the case due to the differences between the model used by the MPC and the simulated one.

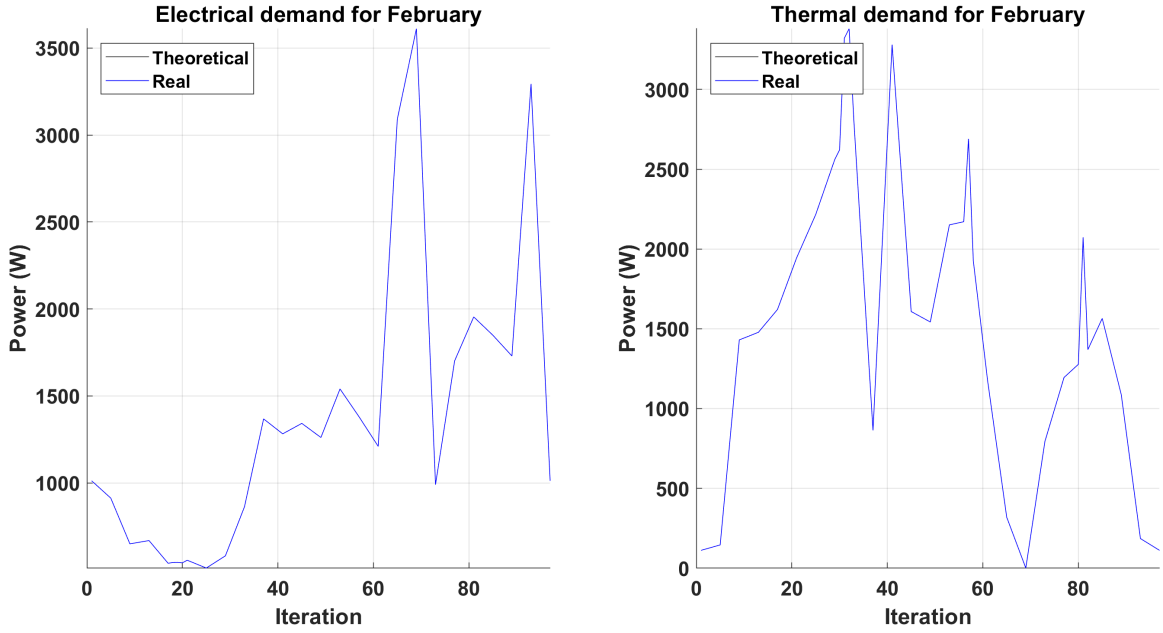

Figure 7.4: Electrical and thermal demand of February.

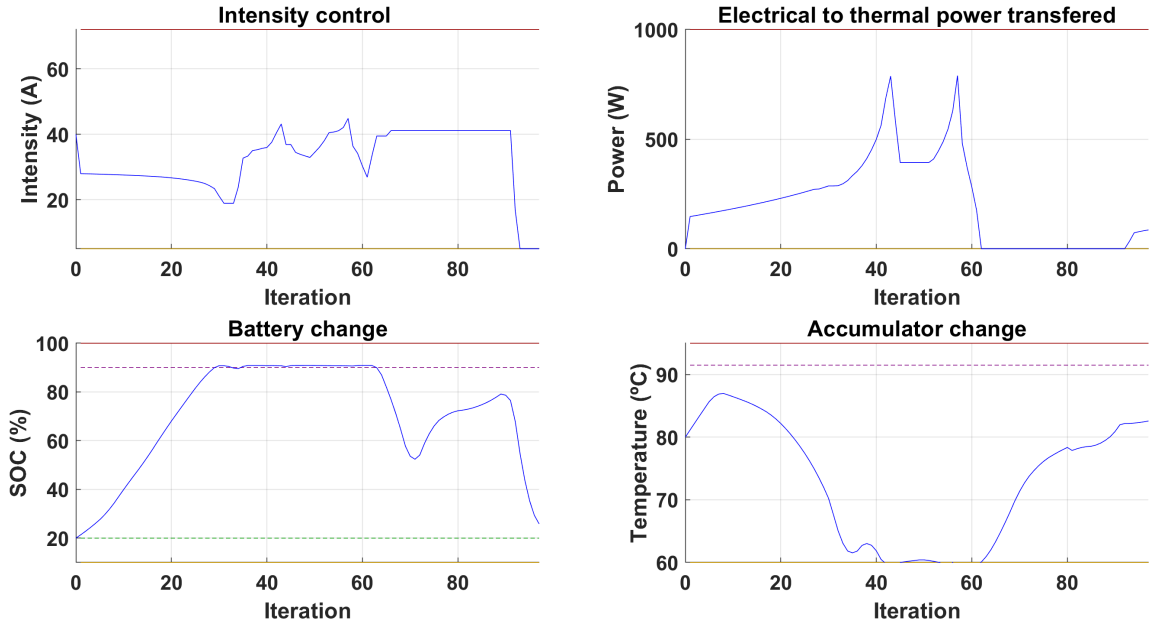

Figure 7.5: Results of the simulation for February.

Additionally, for this test, the simulation done with the linear model has an interesting behaviour, seen in figure 7.6. Similar to the non-linear one, during the last part of the day, the intensity increases trying to give the battery enough energy to avoid going below the lower soft constraint. This however, cannot be avoided as the temperature in the water tank arrives at its maximum allowed point, and therefore, the intensity has to decrease, finishing the simulation at a SoC of 19%.

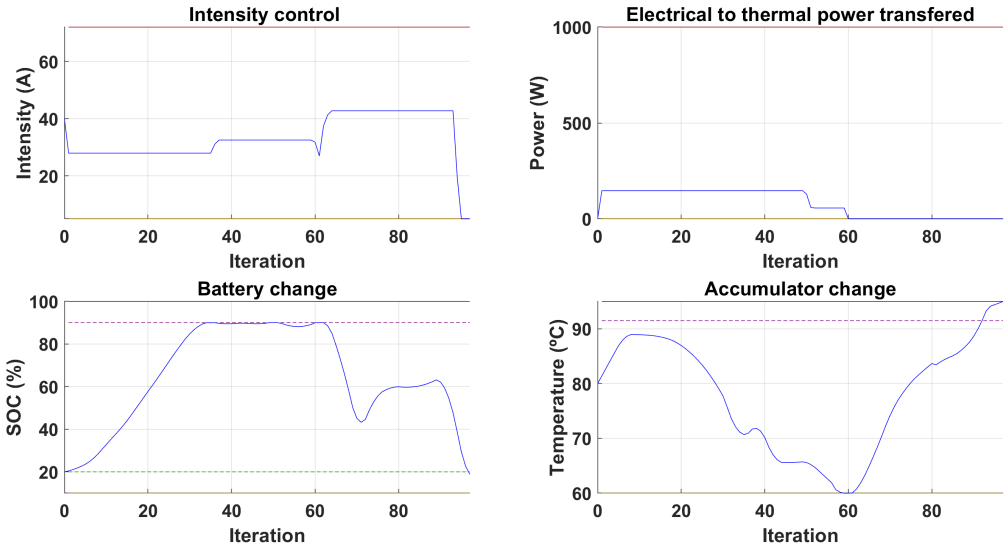

Figure 7.6: Results of the simulation using the linear model.

Here, the behaviour explained in section 5.3.2 can be seen. In this case, the temperature in the water tank shows that there is an excess of thermal energy while decreasing the intensity is an option, this will result in a lack of electrical energy, having to either go below the soft constraints or use the external grid. Therefore, from the three options, the one with the lower weight in the controller will be the one that will be chosen. As the lower one is the soft constraints, the SoC will go below them, not needed neither the external grid nor the accumulator's valve.

Additionally, a simulation has also been done for July. Figure 7.7 shows the demand and figure 7.8 show the fuel cell's intensity along with the transfer power, and the two state variables. This time, the output of hot water has indeed activated, seen in figure 7.9.

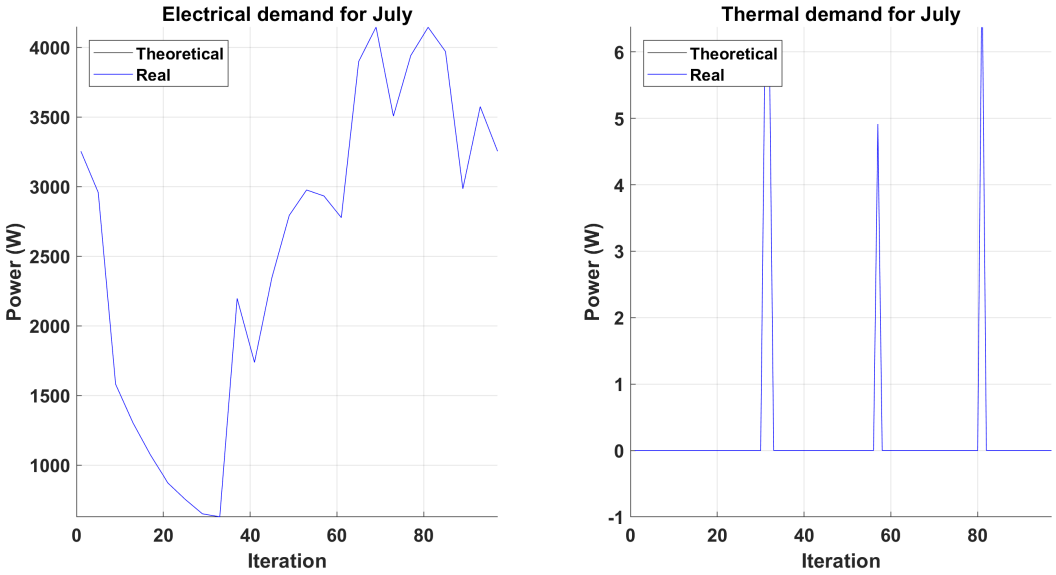

Figure 7.7: Electrical and thermal demand of July.

As the thermal demand of the month is zero at most of the times, the controller focuses on the electrical behaviour of the system, maintaining the transfer resistance at zero and removing the excess of thermal via the valve in the accumulator. This cannot be avoided and it would effectively mean that the fuel cell isn't working in cogeneration, but instead dumping all the generated heat into the environment.

Similar to February, the controller predicts that a lot of electrical power will be needed during the second part of the simulation, and starts to store energy up to the higher soft constraints, maintaining it there until enough has been created, dropping to the lower soft constraint by the end of the day.

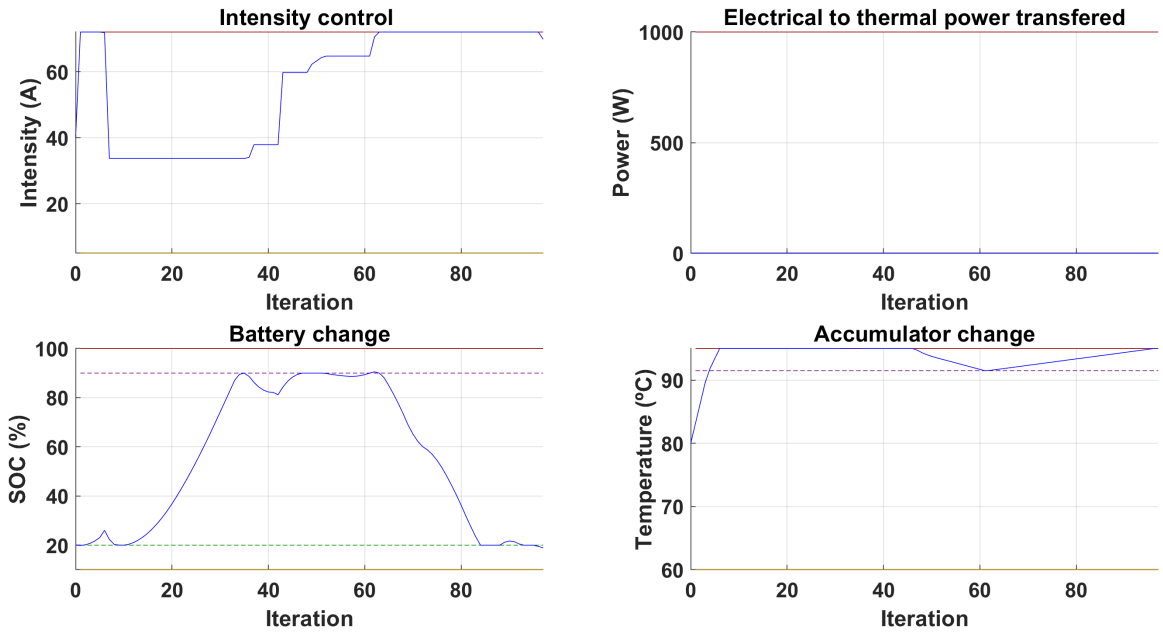

Figure 7.8: Results of the July's simulation.

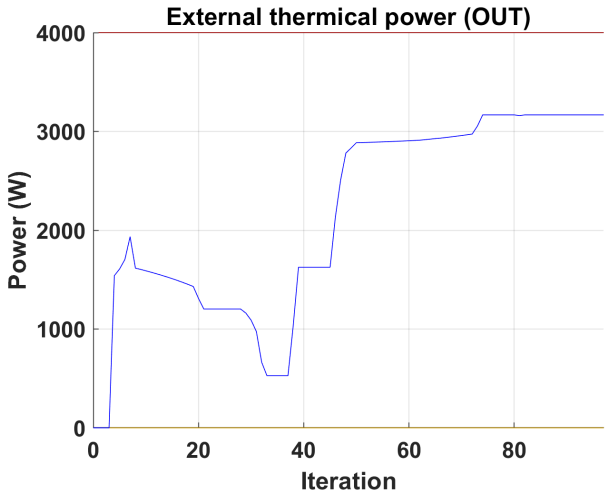

Figure 7.9: Accumulator's valve during July's simulation.

7.4.2 Random real demand

The next simulation has been a more realistic one, where the modelled demand doesn't completely match the real one. To do so, in each iteration, the real demand has been randomly set between 50 and 150% of the modelled one. Figure 7.10 shows the used demand, which is an example of a possible one for November.

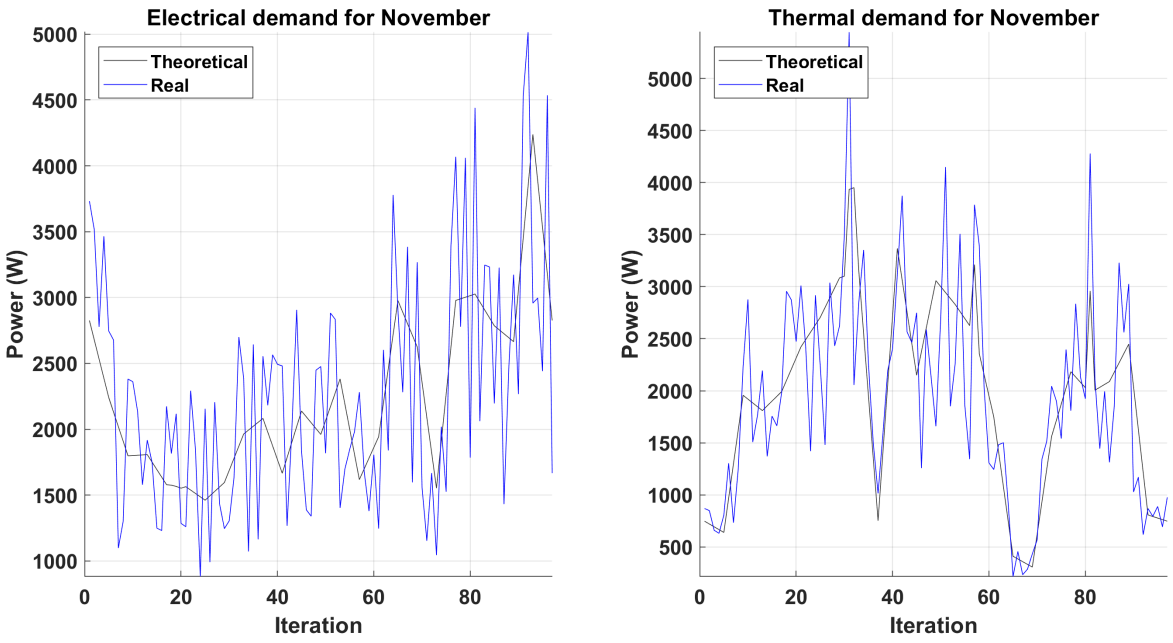

Figure 7.10: Demand used in the simulation.

Seen in figures 7.11 and 7.12, the fuel cell's intensity has been almost constant at around 45 A. Between iterations 50 and 80, the intensity starts to rapidly increase and decrease. This is the result of the missmodelling.

While the controller tries not to break the soft constraint, this different between the expected and the real demand cause a change in the stored energy of the battery. When the real demand is lower, the SoC will increase, going above the soft constraints. As a result, the controller will react, decreasing the fuel cells' intensity in the next iteration. This is repeated over and over again, until around iteration 80, where the SoC starts to go down.

Additionally, the same happens at the start of the simulation, where the differences in demand causes the battery to drop below the soft constraint, Producing a reaction in the controller, setting the intensity at its maximum value.

This shows the importance of soft constraints as if it was a hard one, the controller would have failed, rendering the optimization problem as unfeasible due to the battery's energy being sensored above the limit. This is also seen at the accumulator, where due to the lack of the soft constraints, its security valve has to be activated once.

The connections to the electrical grid where never activated, as there was neither a shortage in electrical energy nor an excess.

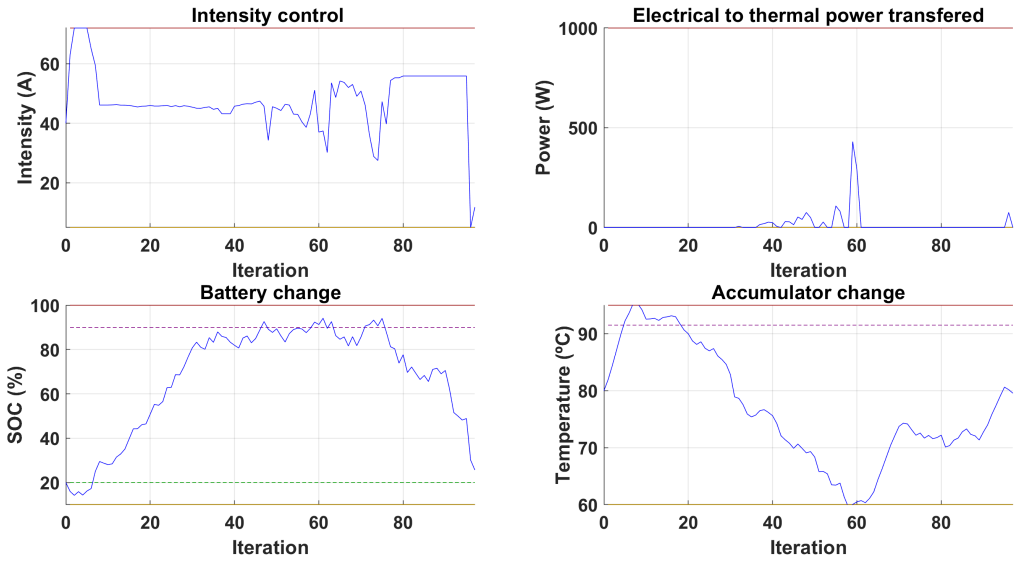

Figure 7.11: Results of the second simulation done.

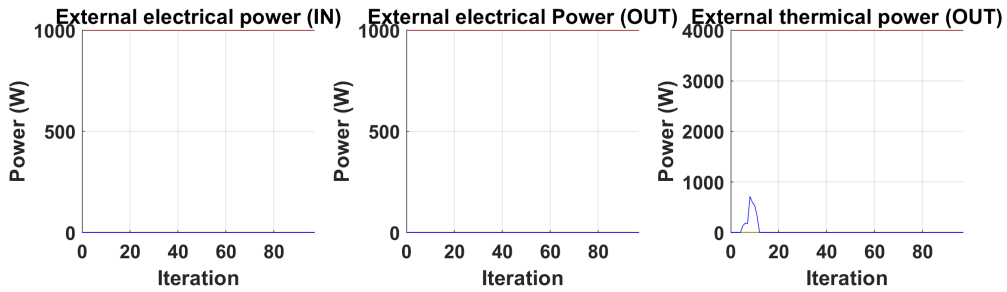

Figure 7.12: Security elements of the system in the missmodelled demand simulation.

7.4.3 Real demand higher than the modelled one

Then, this modelling error has been taken one step further. As this demand is the mean of all the days of the month, and knowing that the difference in temperature's between days can rapidly vary, a new demand was created. This time, the same randomness of the previous one was kept but additionally, 500 W of power were added to all the demand. Figure 7.13 shows the demand used, using April as the base one.

Theoretically, while the real demand is higher than the modelled one, in each iteration, the MPC should be able to adapt to this change, increasing the intensity needed to supply energy to the remaining demand. And due to this change in demand, the higher soft constraints will not be surpassed, while the lower one might.

This behaviour is indeed correct, seen in figures 7.14 and 7.15. At the start, the intensity is slowly increasing, adapting the control to the additional watts consumed. Around midday, the battery reaches its minimum, going below the soft constraints.

Additionally, as the thermal demands is very low, the accumulator's valve will have to extract hot water for most part of the day. The electrical security elements were never activated, as the

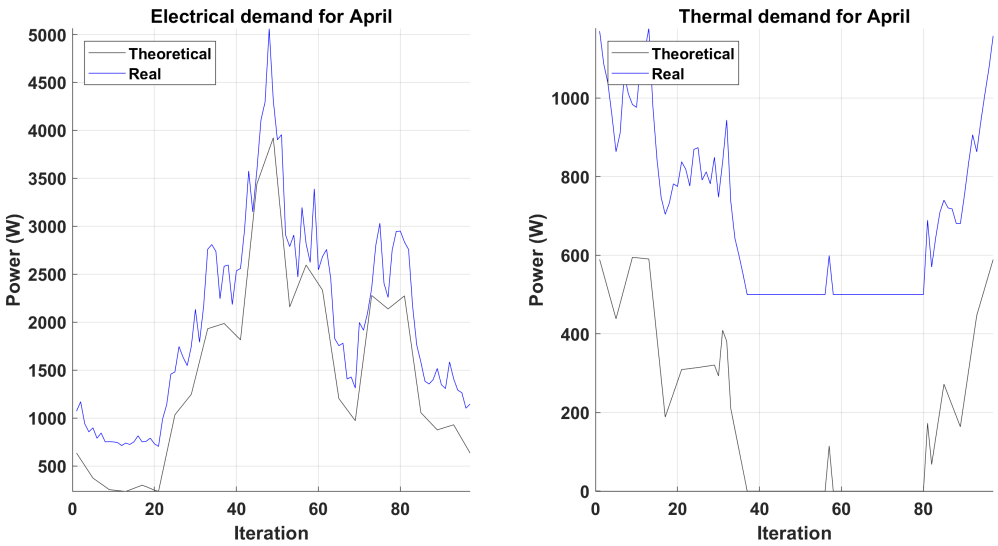

Figure 7.13: Demand used in April's simulation.

soft constraints the electrical power needed could be supplied by the fuel cell alone.

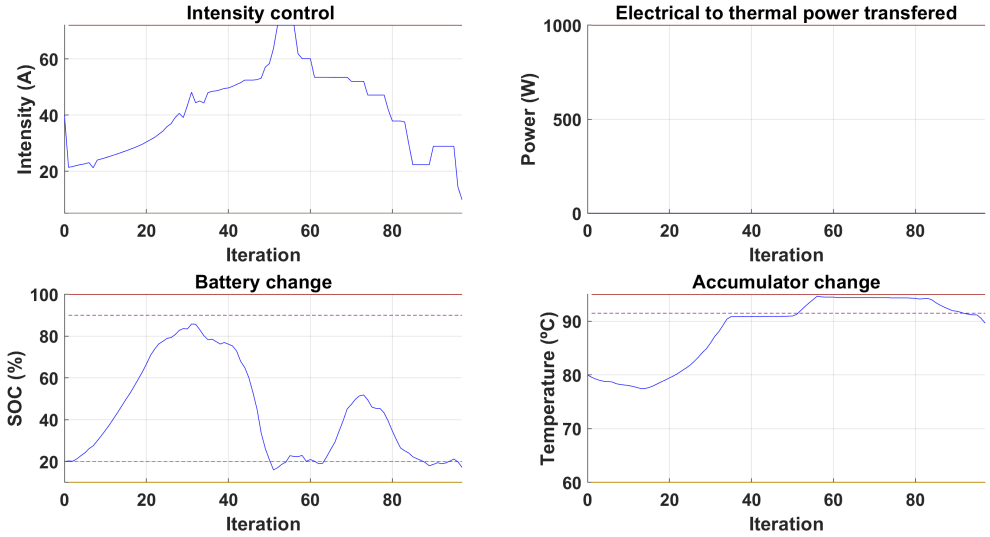

Figure 7.14: Simulation's intensity, accumulator resistance and state space variables.

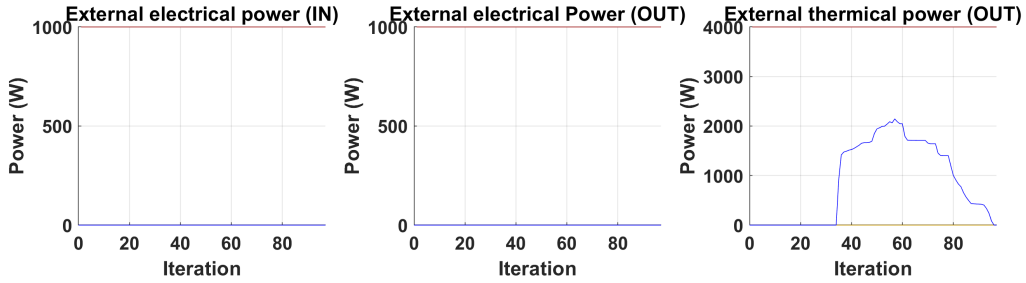

Figure 7.15: Results of the security elements of the system.

7.4.4 Completely different demand

The next scenario is a possible failure in the MPC, where the modelled demand has been taken from another month due to, for example, a software malfunctioning. For this case, the demand can be seen in figure 7.16, being the modelled one, January, and the real one, April. For this arrangement, the electrical demand is modelled very low when in reality it isn't and for the thermal one, the opposite case is applied.

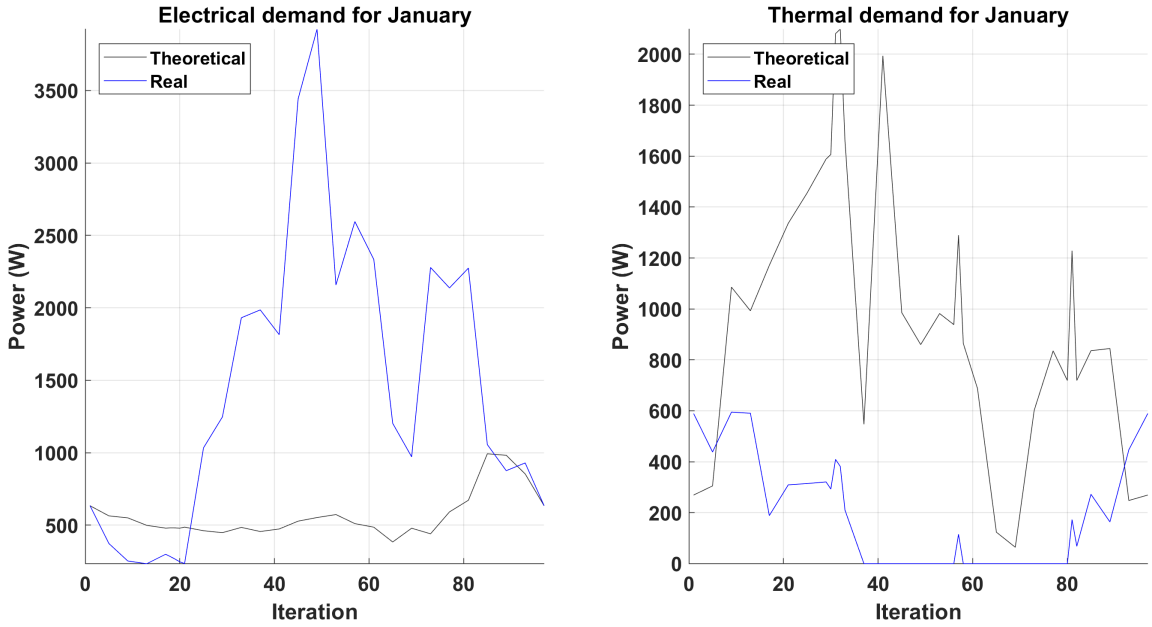

Figure 7.16: Demand used in the simulation with a wrong demand.

Here, taking a look at the electrical part, the intensity falls below the 20 A as the expected demand is very low. At the beginning, the real one is even smaller, and the battery starts storing energy. However, at iteration 20 the demand rapidly increases, draining part of the stored power. The intensity stays the same as the expected one is still low. Twenty iterations later, the battery goes below the soft constraints, which creates a huge change in the fuel cell's intensity.

But this isn't enough, as the modelled demand predicts a lower usage of energy than what really happens. This causes the battery to arrive to its minimum point, having a State of charge of 0%. Fortunately, these high peaks in demand don't last long and the battery's energy increases a bit after that, finishing at the lower constraint.

For the thermal part, as the real one is much smaller than the modelled one, the temperature in the water tank slowly rises at the beginning, where the intensity is small, quickly reaching its maximum value of 95ºC when it increases. From there, the security valve activates, outputting the extra thermal energy.

Additionally, the thermal resistance is activated at the beginning, as a high thermal demand is expected, but is quickly turned off when the battery's energy starts to be drawn. Also, for the electrical security elements, no activation was needed, despite the SOC being below 20% most of the time. This can only be attributed to the low expected electrical demand, which made the

controller suppose that with only the fuel cell's intensity, it would be enough.

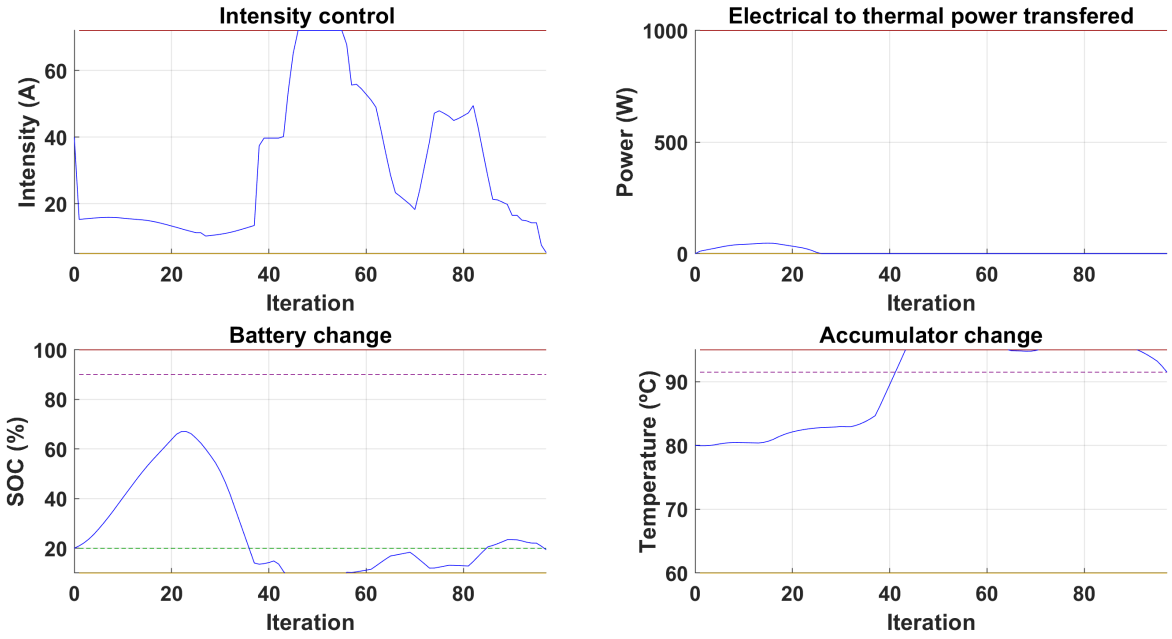

Figure 7.17: Simulation's intensity, accumulator resistance and state space variables.

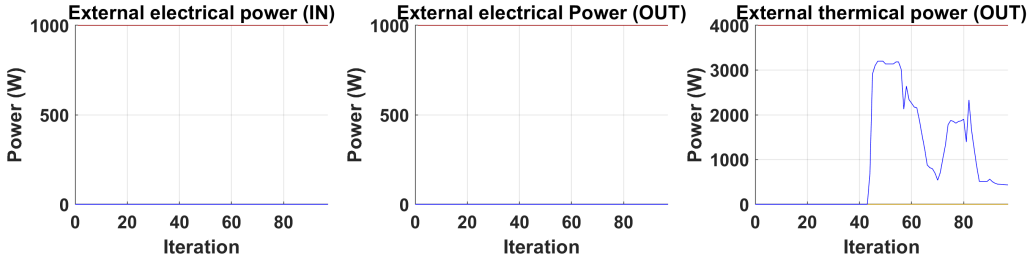

Figure 7.18: Security elements of the simulation with a wrong demand.

7.5 MICAPEM fuel cell comparison

As it was commented when dimensioning the PEMFC, section 4.2.1, these simulations were done using a Horizon 3000W fuel cell. However, close to the end of this thesis, a new one was provided, created by a MICAPEM team. As the final aim of the project is to implemented said fuel cell, both cells will be compared to try to predict the system's behaviour with this new PEMFC.

To do so, the most important parameter that have to be taken into account is the electrical and thermal power generated. Therefore, firstly, the polarization curve will be compared, and then, the electrical power, which can be calculated directly from such curve, and the thermal one.

Figure 7.19 shows the polarization curve and electrical power of the MICAPEM fuel cell and figure 7.20 shows the comparison between the two. For a better view, the intensity has been

scaled into the current density, between 0 and 1, and the voltage, divided by the amount of cells in the stack.

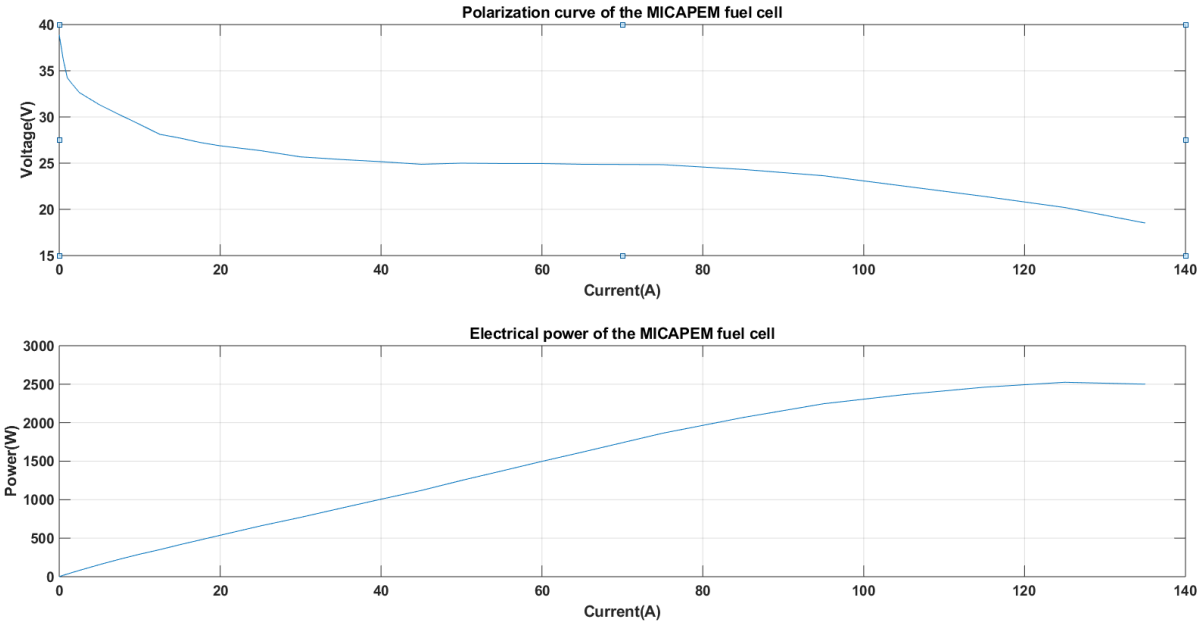

Figure 7.19: Polarization curve and electrical power of the fuel cell created by the MICAPEM.

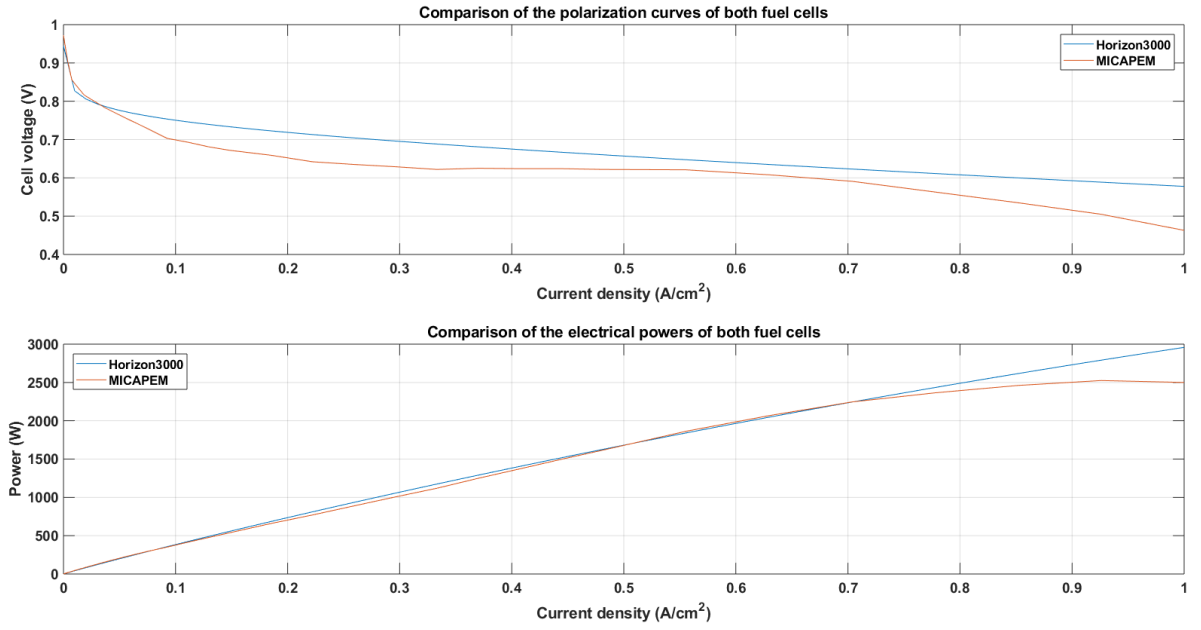

Figure 7.20: Comparison of the polarization curve and electrical power of the Horizon3000 and MICAPEM fuel cell.

From the polarization curve, a difference in intensities can be seen, having the Horizon3000 a maximum of 72 A, whereas the MICAPEM one almost doubles it, with up to 135 A. However, the inverse is seen for the voltage, being around half the value when comparing it to the Horizon3000.

While the polarization curve of the MICAPEM cell has a lower cell voltage than the Horizon3000, the electrical power of both can be considered the same for more than two thirds of the current density. It is only at high enough values that the Horizon3000 is bigger, reaching 3000W, whereas the MICAPEM cell only goes up to 2500 W.

While this is a 17% reduction in power, this will only affect the previous simulations in the moments where the fuel cell is producing an electrical power higher that such value. This translates into an intensity of 60 A or above, and this only happens in two situations.

Firstly, when the SoC of the battery goes below the lower soft constraint. In this cases, this reduction of maximum power wouldn't be a huge concern, as these are punctual situations, lasting very few situations. Instead of creation such high spikes with short duration, the MICAPEM fuel cell will creation smaller one that will last a bit longer.

The other situation is in July. In this case, the fuel cell reaches the 60 A at iteration 50 and doesn't go below that number for the rest of the simulation. In theory, what the fuel cell should do is start storing energy even before the Horizon3000 starts to. This will results in surpassing the higher soft constraints, and for extreme cases, the use of the external grid might be necessary.

For the thermal power, no clear conclusions can be made, as the chemical voltage of this new cell wasn't provided. In general, it can be supposed that if the electrical power of this cell is lower than the Horizon3000's one, then so will the thermal one. This would mean that the intensities would increase. This will result in an increase of thermal power but also of electrical one, resulting in a similar situation than the one just described for July.

However, without the chemical voltage, the exact behaviour is very hard to predict. It is clear however that, specially thanks to the security elements, the system will still be able to supply power to the electrical and thermal demands.

Chapter 8

Economic budget

Regarding the costs of the projects, this has been calculated as a sum of the different types of individual costs. Generally, the costs are divided in three types, intellectual costs, material costs and energy costs. All these will be taken as if this master's thesis was a project done as a service to a company.

When talking about intellectual costs, it is normally referred to as the hours that the people involved in the project have spent. As this master's thesis was done alone, the cost will be the hours spent on the project, which was estimated to be around 560 hours, multiplied by the salary:

Concept	**Salary (€/h)**	**Dedication (h)**	**Total intellectual cost (€)**
Engineer	20	560	**11200**

Table 8.1: Intellectual costs of the master's thesis.

Additionally, the material cost must also be taken into account, including both hardware and software needed to develop the project. In this case, as it was all done via simulations, the only hardware used was a computer, bought specially for this thesis. With a price of 1000€ and an expected duration of 5 years. As the thesis lasted around 6 months, the resulting cost was of 100€.

As for the software, three were used. First of all, Matlab was used, with an annual license of 800€. Then, Yalmip, which is free, and Mosek, that while it is free for academia, commercial uses cost 1950€, with an annual fee of 488€. In total the material costs have been of:

Item	**Cost (€)**
Computer	100
Matlab	400
Mosek	2194
Yalmip	0
TOTAL	**2694**

Table 8.2: Material costs of the master's thesis.

Lastly, the energy costs have to be calculated. In this case, the only energy consumed has been the one used by the computer, which according to different approximations done [24, 25], it will add up to, at most, **100€**.

Therefore, the total cost is of **13994€**, seen in the following table:

Cost type	**Value (€)**
Intelectual	11200
Material	2694
Energy	100
TOTAL	**13994**

Table 8.3: Total cost of the master's thesis.

Chapter 9

Environmental and socioeconomic impact

Lastly, the environmental impact of the project must also be taken into account. As all the results of the project have been taken from simulations, all the project's impact has been the amount of energy consumed by the computer, which is negligible.

Additionally, as part of the MICAPEM project, this thesis can be considered to have a positive environmental impact, as its main object is the implementation of a HT-PEMFC in a house. This will result in the use of an energy source that is both more efficient as well as cleaner, reducing the contamination produced in order to generate the electrical and thermal power.

Moreover, with this project, the creation of a functioning prototype will be created, which will hugely thicken the barrier than fuel cells currently have in the residential section. This will allow the expansion of the use of hydrogen to this sector, resulting in even more cleaner energy sources.

Furthermore, with every project that results in a new viable application for hydrogen, more focus is being drawn into this field, further improving the amount of research carried out.

However, the environmental impact isn't the only impact of this project. As it was just explained, with the creation of a functioning prototype, a new energy source will be available in the houses. This can be compared with the addition of solar panels, but where they are only meant as a support system, the use of fuel cells will completely change the way energy is generated. Adding the need of infrastructures surrounding the fuel cell, such as the supply of hydrogen. this might have an enormous social and economic impact.

Chapter 10

Conclusions

After having analyzed the simulation results, as well as the costs and the impact of this master's thesis, the following conclusions have been taken.

First of all, regarding the use of PEMFCs in cogeneration, the simulation results show that these devices are indeed capable of reliably supplying the energy needed to applications where both electrical and thermal energy are needed. This was seen even in the worst case scenarios, needing only the use of the external grid's power in counted occasions. The output of hot water has been used more often, but this cannot be considered a defect in the system as due to the low thermal energy needed, this was bound to happen.

Moreover, to be able to supply such demand, the architecture developed has only needed the addition of two storing elements as well as an exchanger, which has resulted in a highly simple system.

Additionally, with the use of Model Predictive Control, it has been proofed that not only is the PEMFC capable of supplying the demand but to also minimize the amount of hydrogen used while keeping all the elements of the system in safe conditions.

Lastly, while the initial investment on this system is nowadays expensive, this might soon change due to the research being done in this area. This will result in the availability of hydrogen as a new high efficiency clean energy sources.

Acknowledgments

Before finishing this document, I would like to acknowledge all the help received that made this master's thesis possible.

First of all, I would like to thank my director Ramon Costa for the opportunity to apply part of the learned theory in the master, forming part of a project with the potential to change the paradigms of the energy generation. I would also like to express my gratitude for all the help and guidance received throughout the project without which I wouldn't have arrived this far.

Additionally, appreciate all the effort done by my office colleagues, who have selflessly helped me many times by commenting on the work done, giving suggestions or even helping me when I was stuck in a problem.

Bibliography

[1] H. R. Ellamla, I. Staffell, P. Bujlo, B. G. Pollet, and S. Pasupathi, "Current status of fuel cell based combined heat and power systems for residential sector," *Journal of Power Sources*, vol. 293, pp. 312–328, 2015.

[2] S. Shah, "Advantages and disadvantages of fuel cells applications." url:http://www.greenworldinvestor.com/2018/05/22/advantages-and-disadvantages-of-fuel-cells-applications/.

[3] F. C. T. OFFICE, "Hydrogen storage challenges." url:https://www.energy.gov/eere/fuelcells/hydrogen-storage-challenges.

[4] H. Europe, "Hydrogen storage." url:https://hydrogeneurope.eu/hydrogen-storage.

[5] J. D. Holladay, J. Hu, D. L. King, and Y. Wang, "An overview of hydrogen production technologies," *Catalysis today*, vol. 139, no. 4, pp. 244–260, 2009.

[6] Hydrogen2sys, "Hydrogen." url:https://www.h2sys.fr/en/hydrogen/.

[7] U. D. of Energy, "Hydrogen production and distribution." url:https://afdc.energy.gov/fuels/hydrogen$_production.html$.

[8] M. Ni, D. Y. Leung, M. K. Leung, and K. Sumathy, "An overview of hydrogen production from biomass," *Fuel processing technology*, vol. 87, no. 5, pp. 461–472, 2006.

[9] T. A. of Design, "Fuel cell design." url:https://agencyofdesign.co.uk/projects/fuel-cell-design-1/.

[10] L. Carrette, K. A. Friedrich, and U. Stimming, "Fuel cells: principles, types, fuels, and applications," *ChemPhysChem*, vol. 1, no. 4, pp. 162–193, 2000.

[11] Z. Baroud and A. Benalia, "Steady-state modeling and performance analysis of pem fuel cell," *la 1ère journée d'étude d'automatique et ses applications, LACoSERE, Laghouat*, 2014.

[12] A. Rowe and X. Li, "Mathematical modeling of proton exchange membrane fuel cells," *Journal of power sources*, vol. 102, no. 1-2, pp. 82–96, 2001.

[13] M. Becherif, A. Saadi, D. Hissel, A. Aboubou, and M. Y. Ayad, "Static and dynamic proton exchange membrane fuel cell models," *Journal of Hydrocarbons Mines and Environmental Research*, vol. 2, no. 1, 2011.

[14] X. Huang, Z. Zhang, and J. Jiang, "Fuel cell technology for distributed generation: an overview," in *2006 IEEE International Symposium on Industrial Electronics*, vol. 2, pp. 1613–1618, IEEE, 2006.

[15] M. Knowles, D. Baglee, A. Morris, and Q. Ren, "The state of the art in fuel cell condition monitoring and maintenance," *World Electric Vehicle Journal*, vol. 4, no. 3, pp. 487–494, 2010.

[16] R. H. Tan and L. Y. Hoo, "Dc-dc converter modeling and simulation using state space approach," in *2015 IEEE Conference on Energy Conversion (CENCON)*, pp. 42–47, IEEE, 2015.

[17] J. M. Enrique, A. J. Barragán, E. Durán, and J. M. Andújar, "Theoretical assessment of dc/dc power converters' basic topologies. a common static model," *Applied Sciences*, vol. 8, no. 1, p. 19, 2018.

[18] A. Rahman, N. Fumo, and A. D. Smith, "Simplified modeling of thermal storage tank for distributed energy heat recovery applications," in *ASME 2015 9th International Conference on Energy Sustainability collocated with the ASME 2015 Power Conference, the ASME 2015 13th International Conference on Fuel Cell Science, Engineering and Technology, and the ASME 2015 Nuclear Forum*, pp. V002T13A005–V002T13A005, American Society of Mechanical Engineers, 2015.

[19] T. Alcón Morlas, "Pasteurización de leche con energías renovables en una comunidad rural de cusco (perú)," 2007.

[20] L. Merlin, "Depósito de agua ibc 1000l edd." url:http://www.leroymerlin.es/fp/16438044/deposito-de-agua-ibc-1000l-edd?idCatPadre=244052pathFamilaFicha=3843.

[21] Wikipedia, "Model predictive control." url:https://en.wikipedia.org/wiki/Model$_predictive_control$.

[22] A. Messac, A. Ismail-Yahaya, and C. A. Mattson, "The normalized normal constraint method for generating the pareto frontier," *Structural and multidisciplinary optimization*, vol. 25, no. 2, pp. 86–98, 2003.

[23] R. Toro, C. Ocampo-Martínez, F. Logist, J. Van Impe, and V. Puig, "Tuning of predictive controllers for drinking water networked systems," *IFAC Proceedings Volumes*, vol. 44, no. 1, pp. 14507–14512, 2011.

[24] J. Pablo, "¿cuánta energía gasta un ordenador? (aproximaciones)." url:http://www.leantricity.es/cuanta-energia-gasta-un-ordenador-aproximaciones/.

[25] M. Electricity, "How much electricity does my computer use." url:https://michaelbluejay.com/electricity/computers.html.